REPORT DOCUMENTATION PAGE

1a. REPORT SECURITY CLASSIFICATION Unclassified	**1b. RESTRICTIVE MARKINGS** None
2a. SECURITY CLASSIFICATION AUTHORITY Not Applicable	**3. DISTRIBUTION / AVAIALABILITY OF REPORT** Not Applicable Approved for public release; distribution unlimited.
2b. DECLASSIFICATION / DOWNGRADING SCHEDULE Not Applicable	
4. PERFORMING ORGANIZATION REPORT NUMBER(S) UCB/R/97/A1128	**5. MONITORING ORGANIZATION REPORT NUMBER(S)** AFOSR-TR-97 0318

6a. NAME OF PERFORMING ORGANIZATION Robert O. Ritchie, Dept. of Materials Science & Mineral Engineering	6b. OFFICE SYMBOL (If applicable)	7a. NAME OF MONITORIN Air Force Office of S AFOSR/NA
6c. ADDRESS (City, State, and ZIP Code) University of California, Berkeley 463 Evans Hall # 1760 Berkeley, California 94720-1760		7b. ADDRESS (City, State, 110 Duncan Avenue, Bolling AFB, DC 20332-8080 ATTN: Dr. C. J. Chang
8a. NAME OF FUNDING / SPONSORING ORGANIZATION	8b. OFFICE SYMBOL (If applicable)	9. PROCUREMENT INSTRUMENT IDENTIFICATION NUMBER F49620-96-1-0233

8c. ADDRESS (City, State, and ZIP Code)	10. SOURCE OF FUNDING NUMBERS			
	PROGRAM ELEMENT NO.	PROJECT NO.	TASK NO.	WORK UNIT ACCESSION NO.

11. TITLE (Include Security Classification)
FRACTURE FUNDAMENTALS IN TITANIUM ALUMINIDES (Unclassified)

12. PERSONAL AUTHOR(S)
RITCHIE, R. O. and THOMPSON, A. W.

13a. TYPE OF REPORT Final	13b. TIME COVERED FROM 96/3/1 TO 97/2/28	14. DATE OF REPORT (Year,Month,Day) 1997 June 1	15. PAGE COUNT 39

16. SUPPLEMENTARY NOTATION

17.	COSATI CODES		18. SUBJECT TERMS (Continue on reverse if necessary and identify by block number)
FIELD	GROUP	SUB-GROUP	Intermetallics; Fracture Toughness; Fatigue Crack Propagation; Titanium Aluminides

19. ABSTRACT (Continue on reverse if necessary and identify by block number)

Fracture toughness and fatigue-crack propagation behavior at temperatures between ambient and 800°C has been investigated in a wide range of ($\gamma+\alpha_2$) TiAl microstructures, including single-phase γ, duplex, coarse lamellar (1-2 mm colony size), fine lamellar (~150 μm colony size), and a P/M lamellar microstructure (~65 μm colony size, ~0.1 μm lamellar spacing). The influences of colony size, lamellar spacing and volume fraction of equiaxed γ grains are analyzed in terms of their effects on resistance to the growth of *large* (>5 mm) cracks. Specifically, coarse lamellar microstructures are found to exhibit the best cyclic and monotonic crack-growth properties, while duplex and single-phase γ microstructures exhibit the worst, trends which are rationalized in terms of the salient micromechanisms affecting growth. These mechanisms primarily involve crack-tip shielding (R-curve toughening) processes, and include crack closure, crack deflection, and uncracked ligament bridging. However, since the potency of these mechanisms is severely restricted for cracks with limited wake, in the presence of *small* (<500 μm) cracks the distinction in the fatigue-crack growth resistance of the lamellar and duplex microstructures becomes insignificant. With respect to temperature, resistance to fatigue-crack growth, as characterized by the fatigue threshold, is found to be superior at 800°C, yet inferior at 600°C, compared to room temperature behavior. This "anomalous temperature effect" is ascribed to a dominant role of oxide-induced crack closure at 800°C, which acts to retard near-threshold growth rates and to lead to premature arrest of crack growth at a higher threshold value.

20. DISTRIBUTION / AVAILABILITY OF ABSTRACT ☒ UNCLASSIFIED/UNLIMITED ☐ SAME AS RPT. ☐ DTIC USERS	21. ABSTRACT SECURITY CLASSIFICATION Unclassified	
22a. NAME OF RESPONSIBLE INDIVIDUAL Robert O. Ritchie	22b. TELEPHONE (Include Area Code) (510) 642-0417	22c. OFFICE SYMBOL

DD FORM 1473, 84 MAR — 83 APR edition may be used until exhausted. — SECURITY CLASSIFICATION OF THIS PAGE

All other editions are obsolete.

Unclassified

DTIC QUALITY INSPECTED 4

UNIVERSITY OF CALIFORNIA, BERKELEY
Department of Materials Science and Mineral Engineering

Final Technical Report
to
U.S. Air Force Office of Scientific Research/NA
on

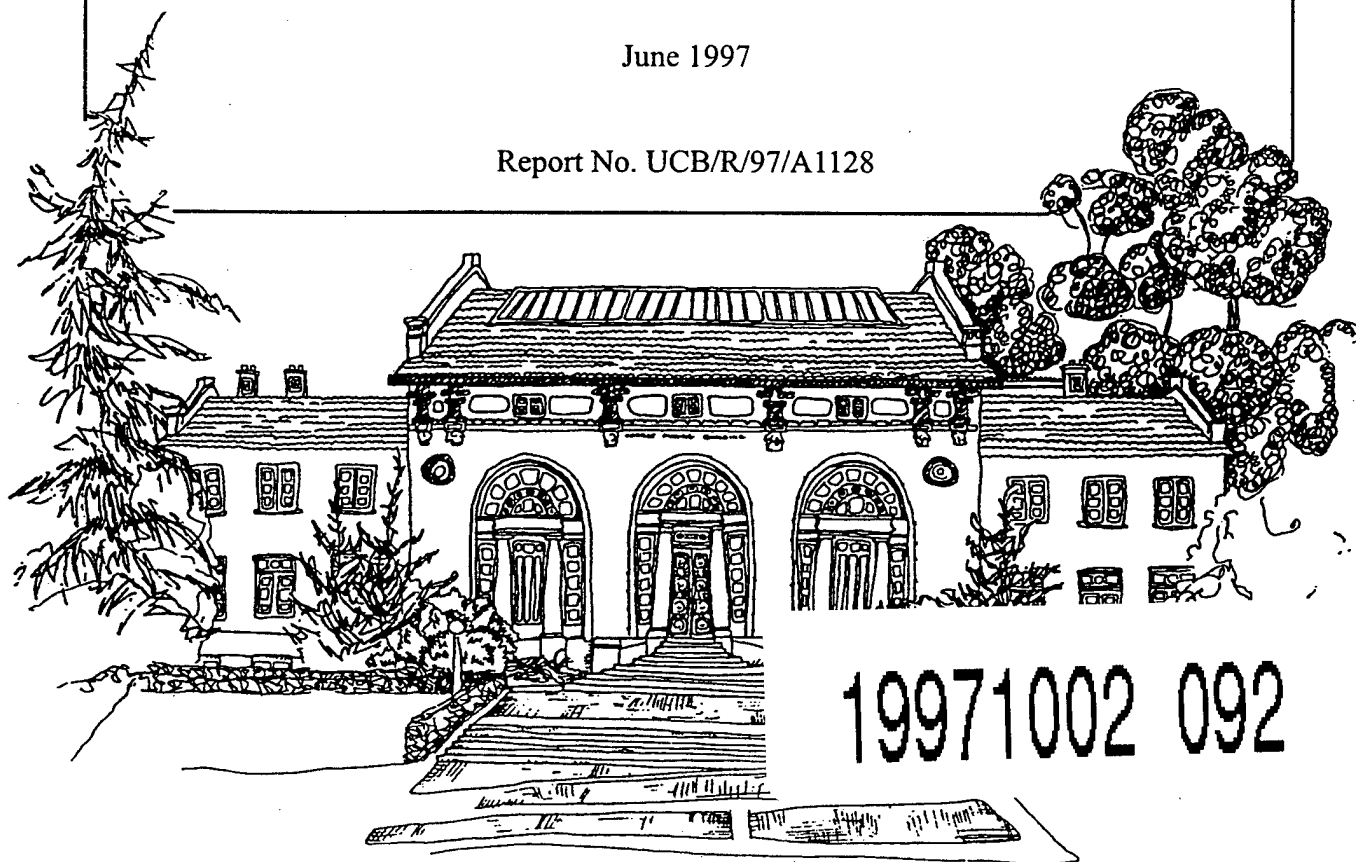# FRACTURE FUNDAMENTALS IN TITANIUM ALUMINIDES

AFOSR Grant No. F49620-96-1-0233

for period 1 March 1996 to 28 February 1997

by

R. O. Ritchie and A. W. Thompson

June 1997

Report No. UCB/R/97/A1128

19971002 092

Final Technical Report

to

U.S. Air Force Office of Scientific Research

on

FRACTURE FUNDAMENTALS IN TITANIUM ALUMINIDES

for period 1 March 1996 to 28 February 1997

submitted to

U.S. Air Force Office of Scientific Research
Directorate of Aerospace and Materials Research
AFOSR/NA
110 Duncan Avenue, Suite B115
Bolling Air Force Base
Washington, D.C.   20322
Attention: Dr. C. J. Chang

submitted by

R. O. Ritchie and A. W. Thompson
Department of Materials Science and Mineral Engineering
University of California, Berkeley, Berkeley, California 94720-1760

June 1, 1997

TABLE OF CONTENTS

FRACTURE FUNDAMENTALS IN TITANIUM ALUMINIDES

R. O. Ritchie and A. W. Thompson

FOREWORD

ABSTRACT

Fracture toughness and fatigue-crack propagation behavior at temperatures between ambient and 800°C has been investigated in a wide range of (γ+α_2) TiAl microstructures, including single-phase γ, duplex, coarse lamellar (1-2 mm colony size), fine lamellar (~150 μm colony size), and a P/M lamellar microstructure (~65 μm colony size, ~0.1 μm lamellar spacing). The influences of colony size, lamellar spacing and volume fraction of equiaxed γ grains are analyzed in terms of their effects on resistance to the growth of *large* (>5 mm) cracks. Specifically, coarse lamellar microstructures are found to exhibit the best cyclic and monotonic crack-growth properties, while duplex and single-phase γ microstructures exhibit the worst, trends which are rationalized in terms of the salient micromechanisms affecting growth. These mechanisms primarily involve crack-tip shielding (R-curve toughening) processes, and include crack closure, crack deflection, and uncracked ligament bridging. However, since the potency of these mechanisms is severely restricted for cracks with limited wake, in the presence of *small* (<500 μm) cracks the distinction in the fatigue-crack growth resistance of the lamellar and duplex microstructures becomes insignificant. With respect to temperature, resistance to fatigue-crack growth, as characterized by the fatigue threshold, is found to be superior at 800°C, yet inferior at 600°C, compared to room temperature behavior. This "anomalous temperature effect" is ascribed to a dominant role of oxide-induced crack closure at 800°C, which acts to retard near-threshold growth rates and to lead to premature arrest of crack growth at a higher threshold value.

1. ON THE ROLE OF MICROSTRUCTURE IN FATIGUE-CRACK GROWTH OF γ-BASED TITANIUM ALUMINIDES

(J. P. Campbell, K. T. Venkateswara Rao, and R. O. Ritchie)

1.1 Introduction

Titanium aluminide intermetallic alloys based on the γ-phase are currently being studied as potential replacements for conventional Ti alloys in gas turbine engines [1-4]. Two classes of microstructure have been prominent: a lamellar structure consisting of colonies, which are generally very coarse in size (~1 to 2 mm), containing alternating γ and α_2 platelets, and a much finer duplex structure consisting of equiaxed grains of γ with small amounts of α_2 or lamellar grains [1]. In general, duplex structures display better elongation and strength, whereas lamellar structures show better toughness and fatigue-crack growth resistance [2,5-8]. Recent research efforts on γ-based titanium aluminides have also focused on variants of the coarse lamellar and fine duplex microstructures, including lamellar structures with refined colony sizes [9], refined lamellae thickness [10], and significant volume fractions of equiaxed γ grains (nearly lamellar microstructures) [9,11]. The effects of these microstructural variations on fracture behavior and fatigue-crack growth are not yet well understood.

This paper presents the results of a study on the room temperature fatigue-crack growth behavior of several dual-phase (γ + α_2) TiAl alloys with a range of microstructures which vary in volume fraction of lamellar colonies and in colony size, including coarse fully lamellar, refined fully lamellar, refined nearly lamellar, and duplex. Comparison of these microstructures indicates that fatigue-crack growth resistance depends strongly upon microstructure. The observed variation in fatigue-crack growth resistance is analyzed in terms of extrinsic crack shielding mechanisms, specifically crack closure and uncracked (shear) ligament bridging.

1.2 Materials and Experimental Methods

Three γ-TiAl intermetallic alloys are examined in the present study. Relevant structural parameters for each microstructure in each alloy are given in Table 1. The first alloy, Ti-47.7Al-2.0Nb-0.8Mn (at.%) containing ~1 vol.% TiB$_2$ particles, was fabricated by the XD™ process, which is a proprietary method for incorporating *in situ* ceramic particulate, whisker or short fiber reinforcements [12]. This alloy was permanent mold cast into 40 mm diameter rods and then hot-isostatic pressed (HIPed) at 1260°C and 172

MPa pressure for 4 hr. The resulting nearly lamellar microstructure (~30% equiaxed γ grains) contained refined lamellar colonies (~120 μm in diameter) (Fig. 1.1a, hereafter referred to as XD nearly lamellar). The TiB$_2$ phase was distributed randomly among γ grains and lamellar colonies as needle-like particles (20-50 μm in length, 2-5 μm in diameter). The second alloy, Ti-47Al-2Nb-2Cr-0.2B (at.%) was processed to yield both a fully lamellar microstructure with refined colony size (~145 μm) (Fig. 1.1b, hereafter referred to as MD fully lamellar) and a duplex microstructure (Fig. 1.1c, hereafter referred to as MD duplex). The third alloy, Ti-47.3Al-2.3Nb-1.5Cr-0.4V (at.%) was treated to yield a fully lamellar microstructure with coarse colony size (~ 1-2 mm) (Fig. 1.1d, hereafter referred to as G7 coarse lamellar) and a duplex microstructure (Fig. 1.1e, hereafter referred to as G7 duplex). The processing details for Ti-47Al-2Nb-2Cr-0.2B and Ti-47.3Al-2.3Nb-1.5Cr-0.4V are presented elsewhere [8,13].

Long (>5 mm) fatigue-crack growth studies were performed in room temperature air on compact tension specimens. Tests were conducted at frequencies of 25 Hz (sine wave) under automated stress-intensity (K) control in general accordance with ASTM Standard E647. A constant load ratio, $R = K_{min}/K_{max}$, of 0.1 (tension-tension) was maintained, where K_{min} and K_{max} are the minimum and maximum stress intensities of the loading cycle. Fatigue thresholds, ΔK_{TH}, were defined as the applied stress-intensity range corresponding to growth rates below ~10^{-10} m/cycle. Crack lengths were monitored using electrical-potential measurements on NiCr foil gauges bonded to the side face of specimens and/or back-face strain compliance methods.

Table 1.1
Microstructure of γ-Based TiAl Alloys

microstructure/ composition (at. %)	lamellar colony size	lamellae spacing*	equiaxed γ phase	γ grain size	yield strength (MPa)
XD nearly lamellar/ Ti-47.7Al-2.0Nb-0.8Mn + 1 vol% TiB$_2$	120 μm	2.0 μm	30%	23 μm	546**
MD fully lamellar/ Ti-47Al-2Nb-2Cr-0.2B	145 μm	1.3 μm	4%	5-20 μm	426
MD duplex/ Ti-47Al-2Nb-2Cr-0.2B	-	-	90%	17 μm	384
G7 coarse lamellar/ Ti-47.3Al-2.3Nb-1.5Cr-0.4V	1-2 mm	1.3 μm	< 5%	10-40 μm	450
G7 duplex/ Ti-47.3Al-2.3Nb-1.5Cr-0.4V	-	-	90-95%	15-40 μm	450

* center-to-center spacing of the α_2 phase
** reported data for a material of similar composition and microstructure [31]

2

Elastic compliance data were also utilized to measure the extent of crack-tip shielding from crack closure and crack bridging. Crack closure was evaluated in terms of the closure stress intensity, K_{cl}, which was approximately defined at the load corresponding to the first deviation from linearity on the unloading compliance [14,15]. Crack bridging was assessed using a method [16] involving a comparison of the experimentally measured unloading compliance (at loads above those associated with closure) with the theoretical value for a traction-free crack in a compact tension sample [17-19]. With this technique, a bridging stress intensity, K_{br}, representing the reduction in K_{max} due to the bridging tractions developed in the crack wake was estimated.

1.3 Results and Discussion

1.3.1 Role of microstructure

The fatigue-crack growth resistance of the XD nearly lamellar, MD fully lamellar, MD duplex, G7 coarse lamellar, and G7 duplex microstructures are compared in Fig. 1.2. Also shown for comparison is the crack growth resistance of a single-phase γ alloy (Ti-55Al (at.%) with traces of Nb, Ta, C, and O) [20] with grain sizes of ~2-10 μm. In general, the lamellar microstructures show superior fatigue-crack growth resistance compared to the equiaxed γ grain materials, i.e. duplex and single-phase γ, consistent with results reported by other authors [4,8,21]. It is interesting to note that the rank ordering of these microstructures in terms of fatigue-crack growth resistance parallels exactly their relative toughness under monotonic loading [9,22]. For all alloys and microstructures, the fatigue-crack growth rates, da/dN, are a strong function of ΔK, particularly for the duplex microstructures, where the entire da/dN(ΔK) curve lies within a ΔK range of ~1 MPa$\sqrt{m}$ or less. Comparatively, the lamellar microstructures show greater damage tolerance, with higher crack-growth thresholds and improved da/dN(ΔK) slopes in the mid-growth rate regime.

The various lamellar microstructures investigated, which differ in lamellar colony size, dimension of the individual lamellae, and volume fraction of equiaxed γ grains, display a range of cyclic crack growth resistance nearly as large as that observed between the lamellar and duplex structures. While the G7 lamellar microstructure, with by far the largest colony size investigated, exhibits the best fatigue-crack growth resistance, the MD fully lamellar material possesses only slightly lower crack-growth resistance despite an order of magnitude reduction in colony size. The difference in crack growth resistance is largest near the threshold; $\Delta K_{TH} = 8.6$ MPa$\sqrt{m}$ for the MD fully lamellar, compared to $\Delta K_{TH} \sim 10$ MPa$\sqrt{m}$ for the coarser G7 structure. The XD nearly lamellar microstructure,

on the other hand, with a colony size (~120 µm) roughly equivalent to that of the MD fully lamellar material (~145 µm), displays significantly lower crack growth resistance. In fact, the XD microstructure shows only marginal improvements in near-threshold fatigue properties (ΔK_{TH} = 7.1 MPa√m) over the equiaxed γ materials (*e.g.* ΔK_{TH} = 6.5 MPa√m and 5.9 MPa√m for the G7 duplex and MD duplex microstructures, respectively), although its fatigue resistance is improved above ~10^{-8} m/cycle. The most prominent microstructural difference between the XD nearly lamellar and MD fully lamellar materials is the high volume fraction (~ 30%) of equiaxed γ grains present in the XD structure. The inferior crack growth behavior of the single-phase γ, G7 duplex, and MD duplex microstructures (Fig. 1.2), all with high volume fractions of equiaxed γ grains, suggests that this morphology of the γ phase may be detrimental to fatigue-crack growth resistance. A deleterious correlation between fatigue-crack growth resistance and equiaxed γ grains is illustrated in Fig. 1.3, where ΔK_{TH} is plotted as a function of the volume fraction of equiaxed γ phase. A similar degradation in toughness due to the presence of the equiaxed γ phase has also been observed [22]. It is believed that the equiaxed γ grains degrade crack growth resistance by inhibiting the activity of extrinsic shielding mechanisms, specifically crack closure (where the γ grains allow for a less tortuous crack path) and uncracked ligament bridging [23,24] (where the γ grains do not participate in uncracked ligament formation).

1.3.2 *Extrinsic crack-tip shielding (crack closure and bridging)*

The disparity in fatigue-crack growth resistance between the duplex and lamellar microstructures and between the various lamellar microstructures can be related to differences in the degree of crack-tip shielding provided by crack closure and uncracked ligament bridges. Fig. 1.4 presents measured K_{cl} for the XD nearly lamellar, MD fully lamellar, and MD duplex structures as a function of ΔK for R = 0.1. Closure stress intensities are highest in the MD fully lamellar microstructure (~ 4-7 MPa√m); however, K_{cl} is greater than K_{min} at all ΔK for each microstructure. There is considerable scatter in the measured K_{cl} for the MD fully lamellar microstructure; however, an increase in K_{cl} with ΔK is observed. This trend is believed to be associated with the formation of uncracked ligament bridges at high ΔK. Although the interpretation of crack closure in the presence of bridging is uncertain, the present results suggest an enhanced closure effect.

It has been well documented [8,24-27] that uncracked ligaments in the crack wake are an important toughening mechanism for monotonic loading in lamellar γ-based TiAl.

4

However, it is often observed that bridging mechanisms, such as ductile phase reinforcements, which are potent under monotonic loading become ineffective during cyclic loading [20,28]. This results from a cyclic degradation of the bridges or from an inability of the bridges to form at the lower stress intensities typical of fatigue (compared to monotonic fracture). In the present study, direct microscopic examination of the crack wake indicates that uncracked ligament bridges can form in lamellar structures during cyclic loading (Fig. 1.5); however, the magnitude of shielding from these ligaments is substantially reduced from that seen under monotonic loading. Indeed previous investigators have reported fractographic evidence of bridge formation during fatigue-crack growth in lamellar TiAl microstructures [29].

The magnitude of shielding provided by uncracked ligaments for both the XD nearly lamellar and MD fully lamellar microstructures was estimated by comparing measured and theoretical unloading compliance [16]. The results are presented in Fig. 1.6, where K_{max}, K_{min}, and K_{max}-K_{br} are plotted as a function of ΔK. The magnitude of shielding provided by uncracked ligament bridging, K_{br}, is given by the difference between the K_{max} and K_{max}-K_{br} lines. Only small amounts of shielding are observed in the XD nearly lamellar TiAl at all ΔK, and in the MD fully lamellar structure at near-threshold loading ($K_{br} \leq 0.5$ MPa$\sqrt{m}$). However, significant shielding does occur in the MD fully lamellar TiAl at higher ΔK, with $K_{br} = 2.1$ MPa$\sqrt{m}$ (14% of K_{max}) at $\Delta K = 12.6$ MPa$\sqrt{m}$. Although substantial, this shielding contribution in fatigue is significantly lower than that which occurs during monotonic fracture, where $K_{br} \sim 4$ to 25 MPa$\sqrt{m}$ [9,30]. The greater propensity for uncracked ligament bridge formation under cyclic loading in the MD fully lamellar microstructure relative to the XD nearly lamellar material is consistent with behavior observed for monotonic loading, as suggested by superior resistance-curve behavior in the MD fully lamellar TiAl [9,22].

Based on the closure and bridging stress intensities presented in Figs. 1.4 and 1.6, the overall crack-tip shielding contribution can be quantified by defining an effective, near-tip stress intensity range, ΔK_{eff}, as follows

$$\Delta K_{eff} = (K_{max} - K_{br}) - K_{cl}, \tag{1}$$

for $K_{cl} > K_{min}$. Plotting the measured fatigue-crack growth rates as a function of the closure and bridging corrected ΔK_{eff} indicates that these shielding mechanisms are largely responsible for the differences in crack growth resistance of the various microstructures. In Fig. 1.7, growth rates are plotted as a function of both the applied stress intensity range, ΔK, and ΔK_{eff} for the MD fully lamellar and MD duplex microstructures (no

shielding from uncracked ligament bridging was measured in the duplex material). For the lamellar microstructure, the shielding correction was applied to crack-growth rates at applied ΔK within 0.5 MPa√m of the stress intensity ranges at which K_{br} was measured. This allowed for plotting a sufficient number of shielding corrected data points; it was assumed that the true values of K_{br} would not vary significantly over this small range of ΔK. After "correcting" for the extrinsic shielding mechanisms, the discrepancy in fatigue-crack growth resistance between the MD fully lamellar and MD duplex microstructures is significantly reduced; the difference in crack growth thresholds is reduced from ~ 3 MPa√m to only ~ 1 MPa√m ($\Delta K_{TH,eff}$ = 4.3 and 5.5 MPa√m, respectively, for the duplex and lamellar structures). These results suggest that the difference in intrinsic fatigue-crack growth resistance between the lamellar and duplex microstructures is small. Affirmation of this point is provided by results reported by Campbell et al. on the growth of small (25-275 µm) fatigue cracks in these same microstructures [13]. Crack-growth rate data sets for small cracks, which are far less affected by shielding contributions due to their limited wake, show considerable scatter in the MD fully lamellar and MD duplex microstructures, but essentially overlap.

The range of crack-growth resistance exhibited by the various lamellar microstructures can also be attributed in part to extrinsic crack-tip shielding. In Fig. 1.8, crack-growth rates in the XD nearly lamellar and MD fully lamellar microstructures are plotted both as a function of the applied ΔK and the closure and shielding corrected ΔK_{eff}. The discrepancy in crack-growth resistance between the two microstructures is virtually eliminated when da/dN are plotted as a function of ΔK_{eff}, particularly in the near-threshold regime, with $\Delta K_{TH,eff}$ = 5.5 MPa√m for both materials. The scatter at higher growth rates for the shielding-corrected data in the MD fully lamellar microstructure results from scatter in the measured K_{cl} (Fig. 1.4).

Clearly, comparisons between the various lamellar and duplex microstructures based on "long-crack" fatigue-crack growth properties (Fig. 1.2) indicate that the coarser lamellar structures are superior. However, such improved crack-growth resistance has been shown to result primarily from extrinsic shielding mechanisms (bridging and closure) which operate behind the crack tip. Considering the steep slope of the $da/dN(\Delta K)$ curves exhibited by these intermetallic alloys, for many fatigue critical applications the fatigue threshold in the presence of small cracks (where shielding is ineffective) may well be a critical design parameter. Under these design specifications, the duplex microstructures exhibit performance nearly equivalent to that of lamellar microstructures. In fact, in the fatigue-limited applications for which γ-based titanium

6

aluminides are being considered, the duplex structures may well be superior as they display higher (smooth bar) fatigue limits [4] and, due to their finer microstructures, small-crack growth rates are prone to far less scatter [13].

1.4 Conclusions

Based on a study of room temperature fatigue-crack growth in a wide range of γ-based TiAl alloys and microstructures, including duplex, fully lamellar with coarse colony size, fully lamellar with refined colony size, and nearly lamellar with refined colony size, the following conclusions can be made:

1. Fatigue-crack growth resistance depends strongly on microstructure. In general, lamellar microstructures exhibit superior damage tolerance, with higher crack-growth thresholds, ΔK_{TH}, and improved $da/dN(\Delta K)$ slopes in the mid-growth rate regime, when crack growth is characterized in terms of long (>5 mm) crack behavior and the far-field (applied) stress intensity range.

2. The discrepancy in fatigue-crack growth resistance between lamellar and duplex microstructures in Ti-47Al-2Nb-2Cr-0.2B (at.%) can largely be attributed to higher crack-tip shielding (from closure and bridging) in the lamellar structure. Variations in the degree of shielding provided by these extrinsic toughening mechanisms are also responsible for some of the discrepancy in fatigue-crack growth resistance between the various lamellar microstructures investigated.

3. A deleterious correlation is observed between fatigue-crack growth resistance and the presence of equiaxed γ grains. It is believed that the equiaxed γ phase degrades crack growth resistance by inhibiting the action of crack closure and uncracked ligament bridging.

4. Given that the superior fatigue-crack growth resistance of the lamellar microstructure in Ti-47Al-2Nb-2Cr-0.2B (at.%) can be largely attributed to extrinsic toughening mechanisms which act in the crack wake, it is expected (and has been observed [13]) that fatigue-crack growth resistance in the presence of small cracks, which are not significantly influenced by extrinsic crack shielding due to their limited wake, will be comparable in the lamellar and duplex microstructures.

1.5 References

1. Y.W. Kim, *JOM* **46**(7) (1994) 30.

2. Y.-W. Kim and D.M. Dimiduk, *JOM* **43**(8) (1991) 40.

3. G.F. Harrison and M.R. Winstone, in *Mechanical Behavior of Materials at High Temperature*, C. Moura Branco, R.O. Ritchie and V. Sklenicka (eds.), Kluwer Academic Publishers: NATO ASI Series, 1996, p. 309.

4. J.M. Larsen, B.D. Worth, S.J. Balsone and J.W. Jones, in *Gamma Titanium Aluminides*, Y.-W. Kim, R. Wagner and M. Yamaguchi (eds.), TMS, Warrendale PA, 1995, p. 821.

5. K.S. Chan, *Metall. Trans.* **24A** (1993) 569.

6. K.S. Chan and Y.-W. Kim, *Metall. Trans.* **23A** (1992) 1663.

7. K.S. Chan and Y.-W. Kim, *Metall. Trans.* **24A** (1993) 113.

8. K.T. Venkateswara Rao, Y.-W. Kim, C.L. Muhlstein and R.O. Ritchie, *Mater. Sci. Eng.* **A192** (1995) 474.

9. J.P. Campbell, A.L. McKelvey, S. Lillibridge, K.T. Venkateswara Rao and R.O. Ritchie, in *Deformation and Fracture of Ordered Intermetallic Materials IV: Titanium Aluminides*, W.O. Soboyejo, T.S. Srivatsan and H.L. Fraser (eds.), TMS, Warrendale PA, 1997, p. 141.

10. C.T. Liu, P.J. Maziasz, D.R. Clemens, J.H. Schneibel, V.K. Sikka, T.G. Nieh, J. Wright and L.R. Walker, in *Gamma Titanium Aluminides*, Y.-W. Kim, R. Wagner and M. Yamaguchi (eds.), TMS, Warrendale PA, 1995, p. 679.

11. G. Malakondaiah and T. Nicholas, *Metall. Mater. Trans.* **27A** (1996) 2239.

12. K.S. Kumar, J.A.S. Green, J. D.E. Larsen and L.D. Kramer, *Adv. Mater. Proc.* **148**(4) (1995) 35.

13. J.P. Campbell, J.J. Kruzic, S. Lillibridge, K.T. Venkateswara Rao and R.O. Ritchie, *Scripta Mater.* **36** (1997) in press.

14. W. Elber, *Eng. Fract. Mech.* **2** (1970) 37.

15. R.O. Ritchie and W. Yu, in *Small Fatigue Cracks*, R.O. Ritchie and J. Lankford (eds.), TMS-AIME, Warrendale, PA, 1986, p. 167.

16. R.O. Ritchie, W. Yu and R.J. Bucci, *Eng. Fract. Mech.* **32** (1989) 361.

17. W.F. Deans and C.E. Richards, *J. Test. Eval.* **7** (1979) 147.

18. C.E. Richards and W.F. Deans in *The Measurement of Crack Length and Shape During Fracture and Fatigue*, C.J. Beevers (ed.), EMAS Ltd., Warley, UK, 1980, p. 28.

19. D.C. Maxwell, in *Materials Laboratory, Air Force Wright Aeronautical Laboratories, Report No. AFWAL-TR-87-4046*, Wright-Patterson Air Force Base, Dayton, OH, 1987.

20. K.T. Venkateswara Rao, G.R. Odette and R.O. Ritchie, *Acta Metall. Mater.* **42** (1994) 893.

21. S.J. Balsone, J.M. Larsen, D.C. Maxwell and J.W. Jones, *Mater. Sci. Eng.* **A192/193** (1995) 457.

22. J.P. Campbell, K.T. Venkateswara Rao and R.O. Ritchie, *Metall. Mater. Trans.* (1997) in review.

23. K.S. Chan, *Metall. Trans.* **22A** (1991) 2021.

24. K.S. Chan, *JOM* **44**(5) (1992) 30.

25. K.S. Chan and Y.-W. Kim, *Metall. Mater. Trans.* **25A** (1994) 1217.

26. K.S. Chan and Y.-W. Kim, *Acta Metall. Mater.* **43** (1995) 439.

27. H.E. Dève, A.G. Evans and D.S. Shih, *Acta Metall. Mater.* **40** (1992) 1259.

28. D.R. Bloyer, K.T. Venkateswara Rao and R.O. Ritchie, in *Layered Materials for Structural Applications*, J.J. Lewandowski, C.H. Ward, M.R. Jackson and J.W. Hunt, Jr. (eds.), MRS, Pittsburgh PA, 1996, p. 243.

29. D.J. Wissuchek, G.E. Lucas and A.G. Evans, in *Gamma Titanium Aluminides*, Y.-W. Kim, R. Wagner and M. Yamaguchi (eds.), TMS, Warrendale PA, 1995, p. 875.

30. K.S. Chan, *Metall. Mater. Trans.* **26A** (1995) 1407.

31. D.E. Larsen, in *Microstructure/ Property Relationships in Titanium Aluminides and Alloys*, Y.-W. Kim and R. R. Boyer (eds.), TMS, Warrendale PA, 1991, p. 345.
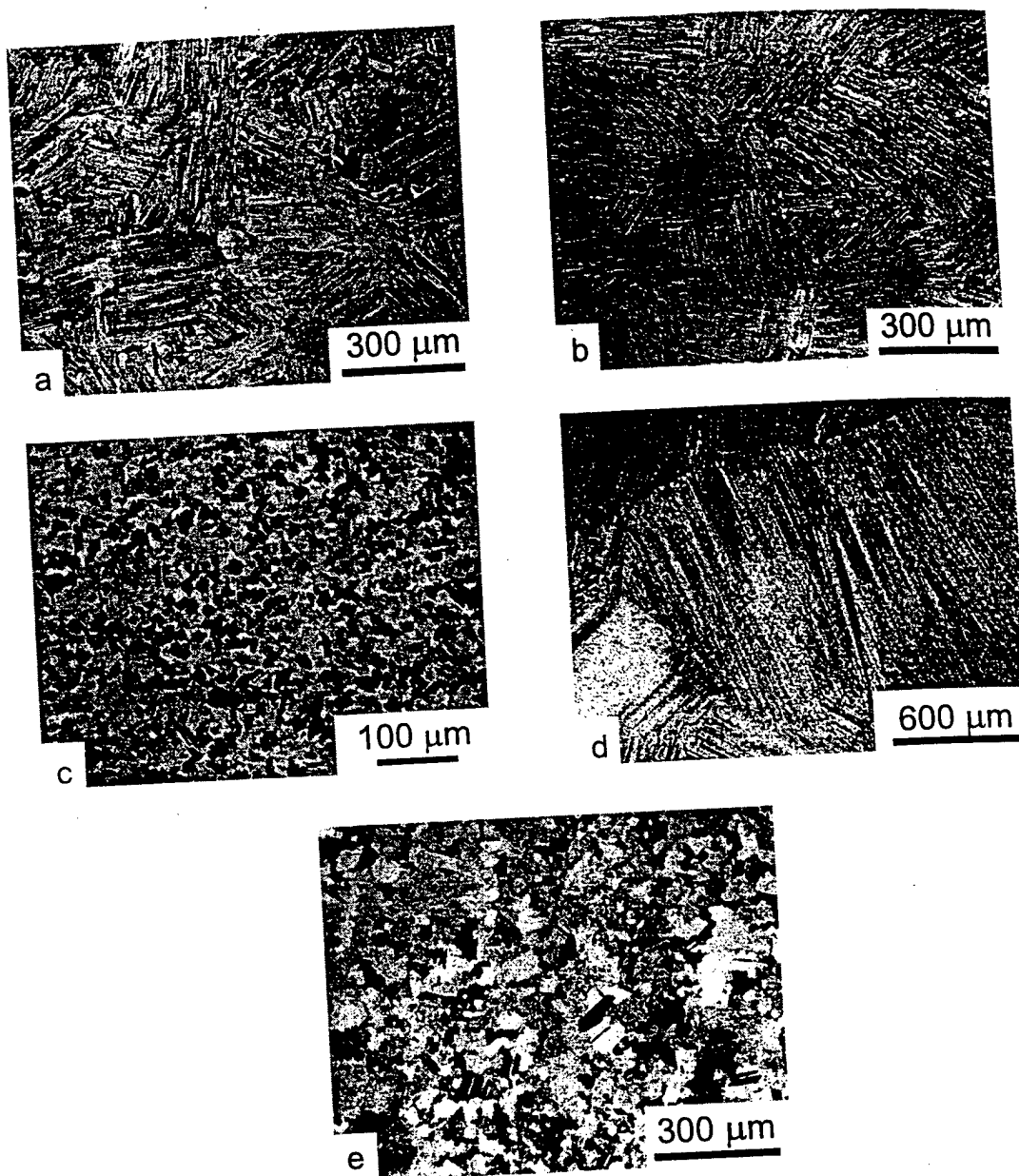
Fig. 1.1: Optical micrographs of (a) Ti-47.7Al-2.0Nb-0.8Mn + 1 vol.% TiB_2 (XD nearly lamellar), (b) Ti-47Al-2Nb-2Cr-0.2B (MD fully lamellar), (c) Ti-47Al-2Nb-2Cr-0.2B (MD duplex), (d) Ti-47.3Al-2.3Nb-1.5Cr-0.4V (G7 coarse lamellar), and (e) Ti-47.3Al-2.3Nb-1.5Cr-0.4V (G7 duplex) microstructures.
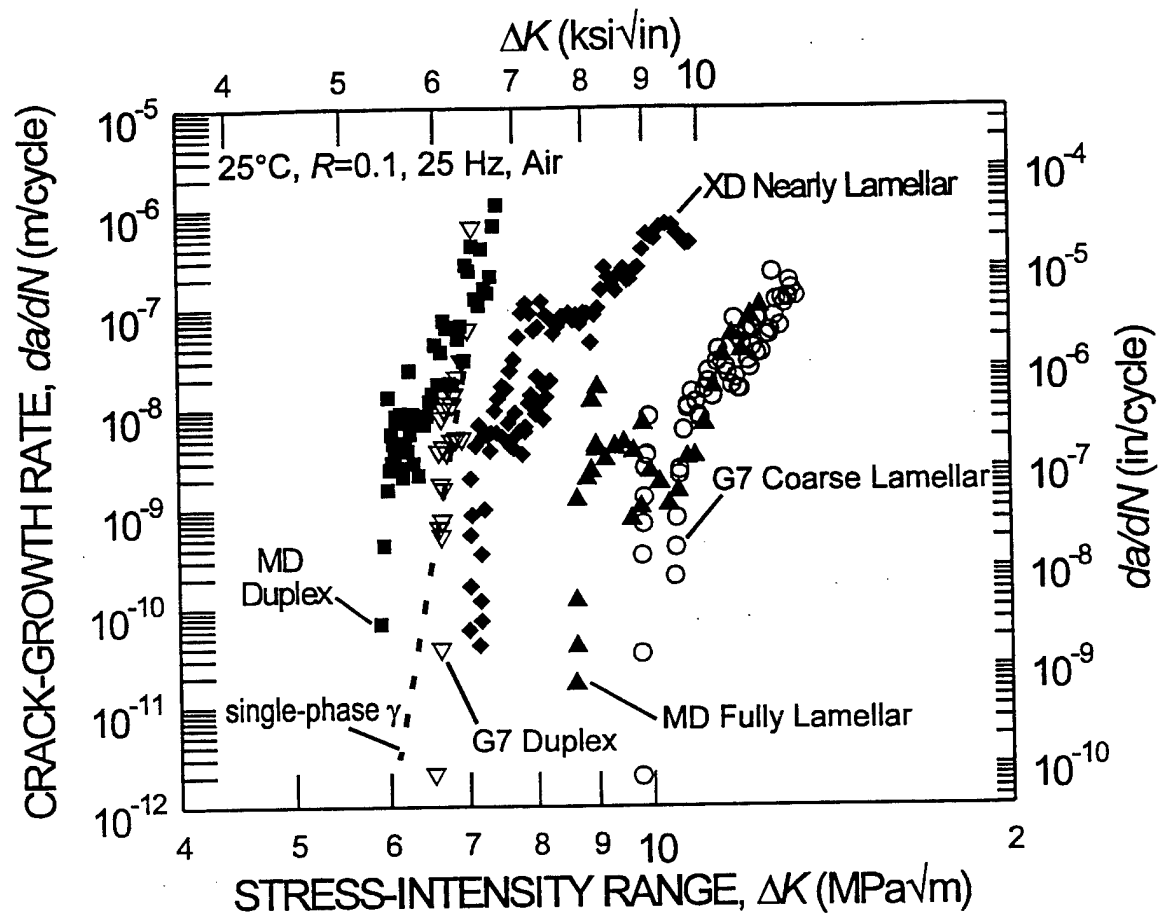
Fig. 1.2: Room temperature fatigue-crack growth resistance in G7 coarse lamellar, G7 duplex, MD fully lamellar, MD duplex, XD nearly lamellar, and single-phase γ microstructures. In general the lamellar microstructures show superior fatigue-crack growth resistance compared to the equiaxed γ structures (*i.e.* duplex and single-phase γ). The various lamellar microstructures investigated display a range of cyclic crack growth resistance nearly as large as that observed between the lamellar and duplex structures.
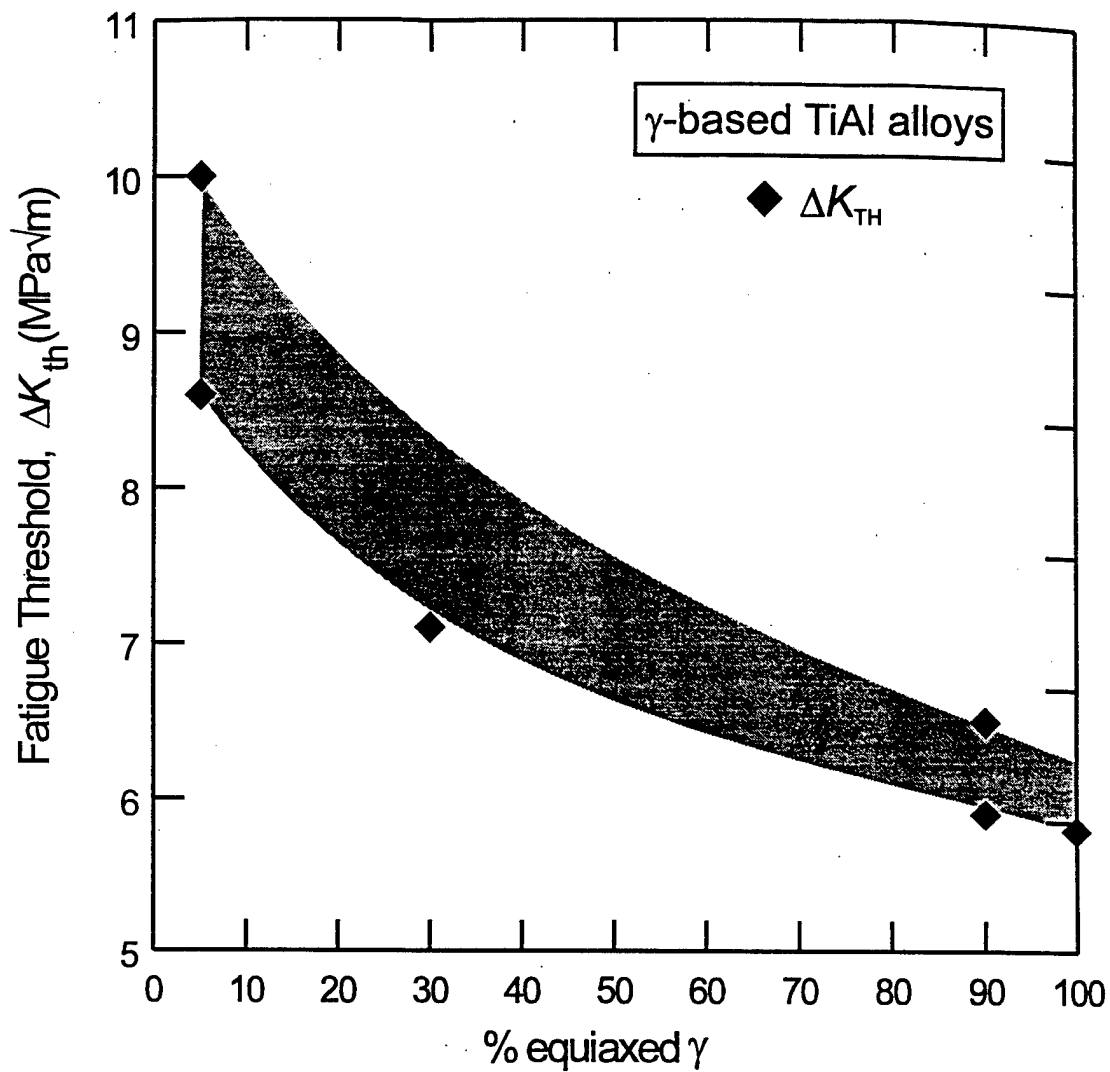
Fig. 1.3: The fatigue threshold, ΔK_{TH}, as a function of the volume fraction of equiaxed γ grains in several γ-based TiAl microstructures (XD nearly lamellar, MD fully lamellar, MD duplex, G7 coarse lamellar, G7 duplex, and single-phase γ). A deleterious correlation between fatigue-crack growth resistance and the equiaxed γ phase is observed.

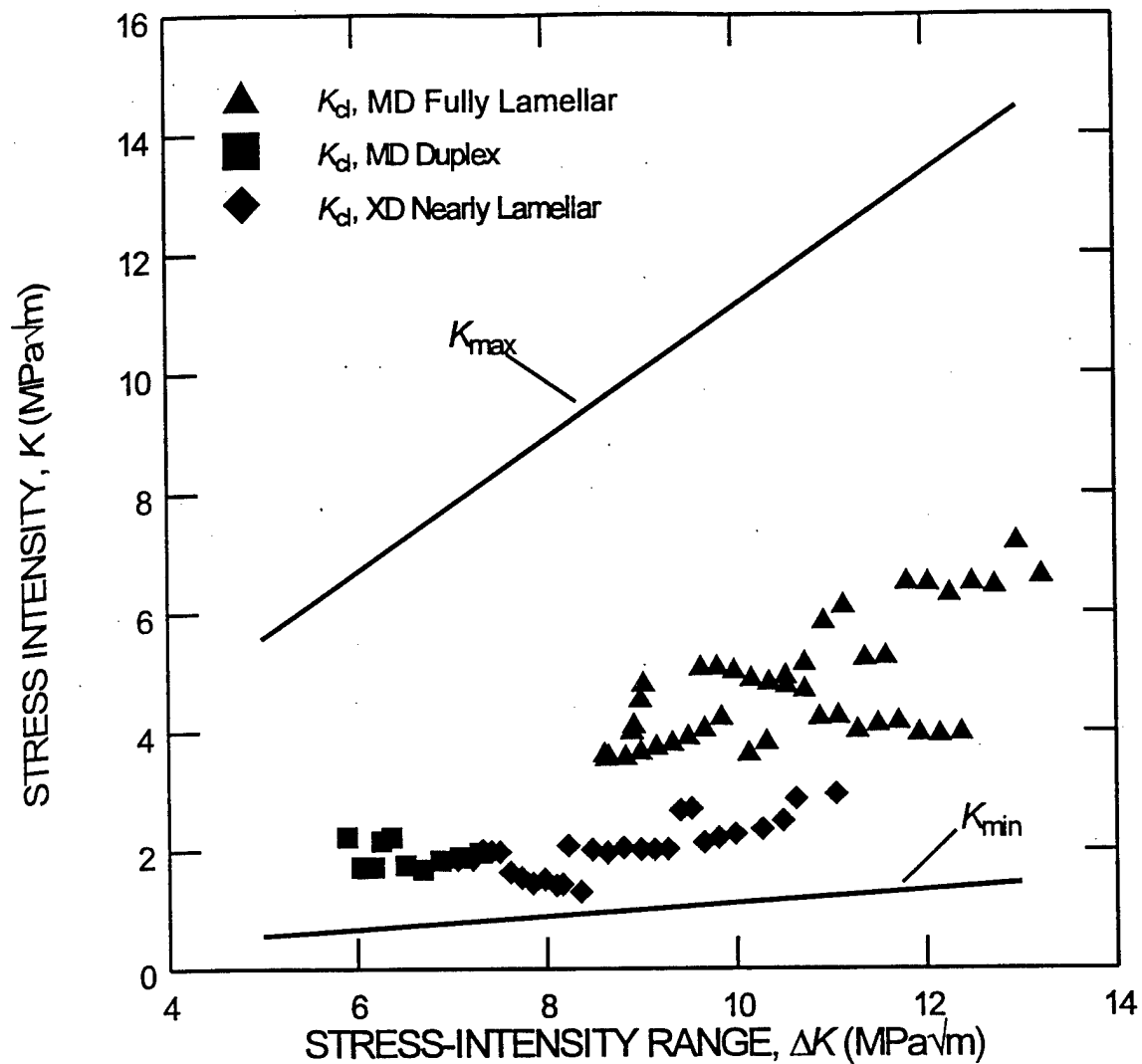Fig. 1.4: Measured crack closure stress intensities, K_{cl}, as a function of ΔK ($R = 0.1$) in the MD fully lamellar, MD duplex, and XD nearly lamellar microstructures. Solid lines indicating K_{max} and K_{min} are also presented. K_{cl} is observed to be largest in the MD lamellar microstructure (~ 4-7 MPa√m), however $K_{cl} > K_{min}$ for all microstructures at all ΔK levels.

Crack Growth Direction
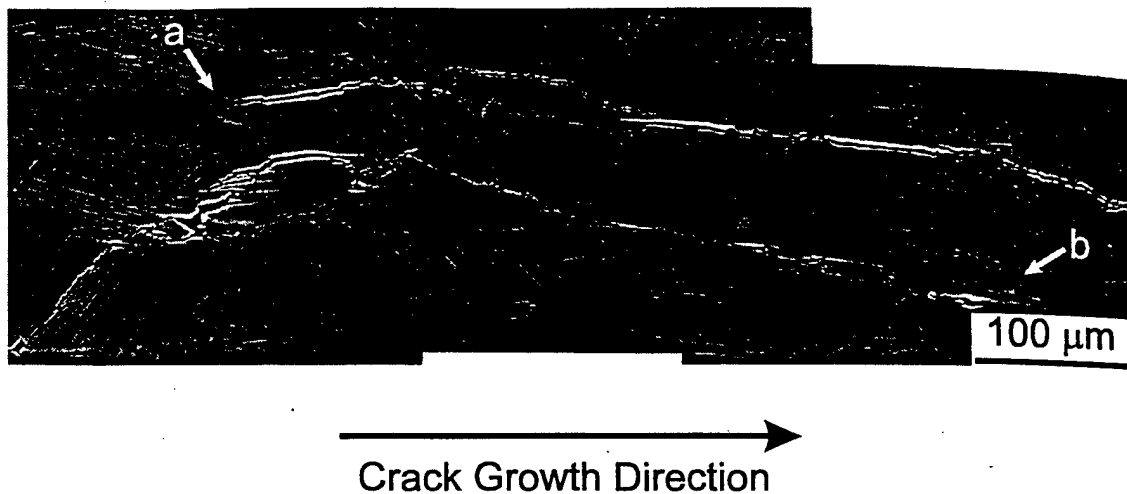
Fig. 1.5: Scanning electron micrograph of a fatigue-crack profile in the MD fully lamellar microstructure (recorded at sample mid-thickness) showing the presence of uncracked ligament bridges. The arrows **a** and **b** indicate the beginning of the crack at the top of the bridge and the end of the crack at the bottom of the bridge, respectively. This region of the sample was tested at a constant ΔK of 12.5 MPa$\sqrt{}$m ($R = 0.1$).
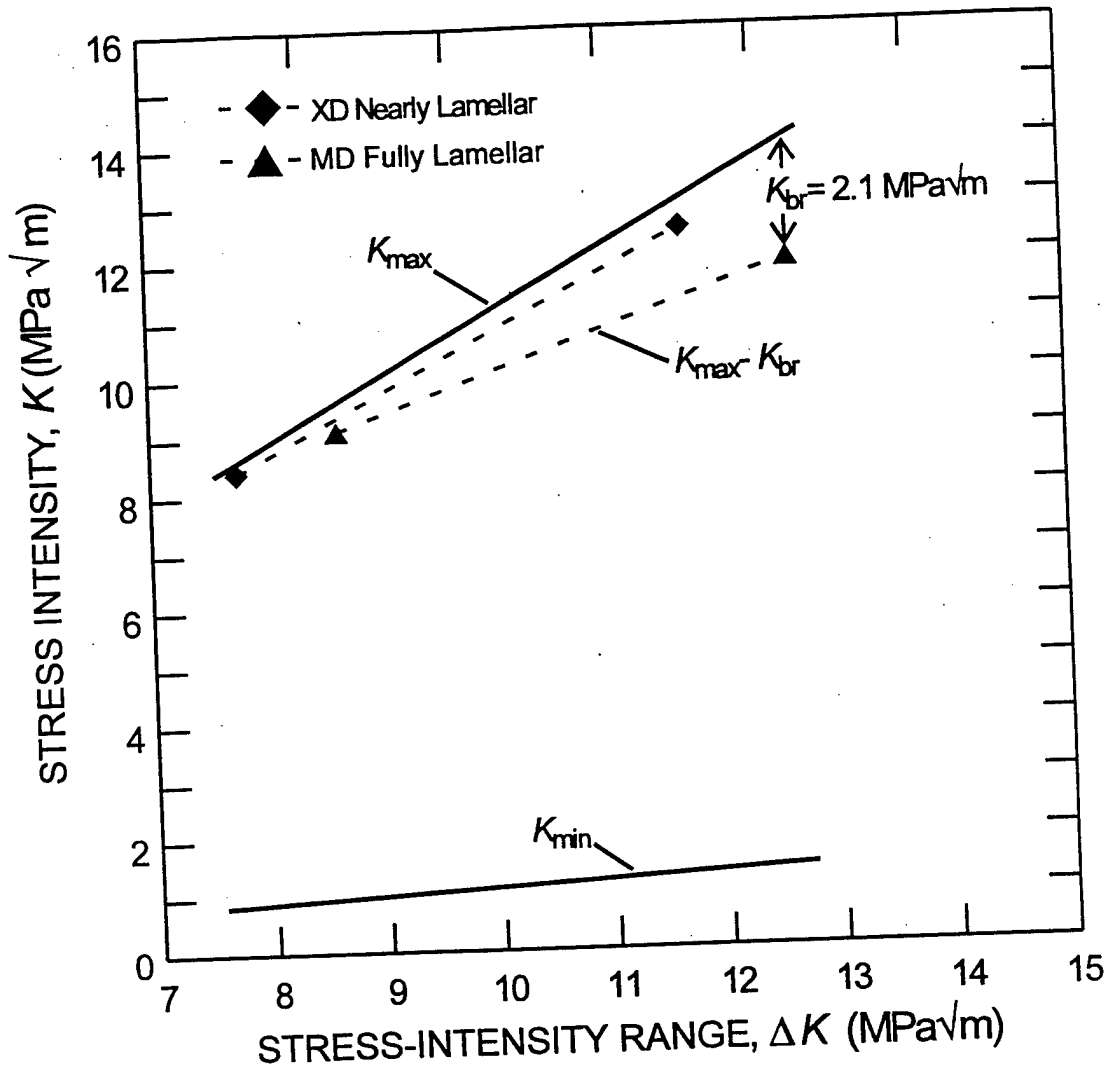
Fig. 1.6: K_{max}, K_{min}, and K_{max}-K_{br} as a function of ΔK ($R = 0.1$) for the MD fully lamellar and XD nearly lamellar microstructures. The magnitude of shielding provided by uncracked ligament bridging, K_{br}, is given by the difference between the K_{max} and K_{max}-K_{br} lines. Only small amounts of shielding are observed in the XD nearly lamellar TiAl ($K_{br} \sim 0.2$ - 0.5 MPa√m). Significant shielding does occur in the MD fully lamellar TiAl at higher ΔK, with $K_{br} = 2.1$ MPa√m (14% of K_{max}) at $\Delta K = 12.6$ MPa√m.

Fig. 1.7: Fatigue-crack growth rates, *da/dN*, for long cracks in the MD fully lamellar and MD duplex microstructures are plotted as a function of the applied stress intensity range, ΔK, and an effective, near-tip stress intensity range, ΔK_{eff}, from which the effect of extrinsic crack shielding mechanisms (closure and bridging) have been "subtracted". It is apparent that these extrinsic shielding mechanisms are largely responsible for the disparity in fatigue-crack growth resistance between the two microstructures which is observed when crack-growth rates are plotted as a function of ΔK.
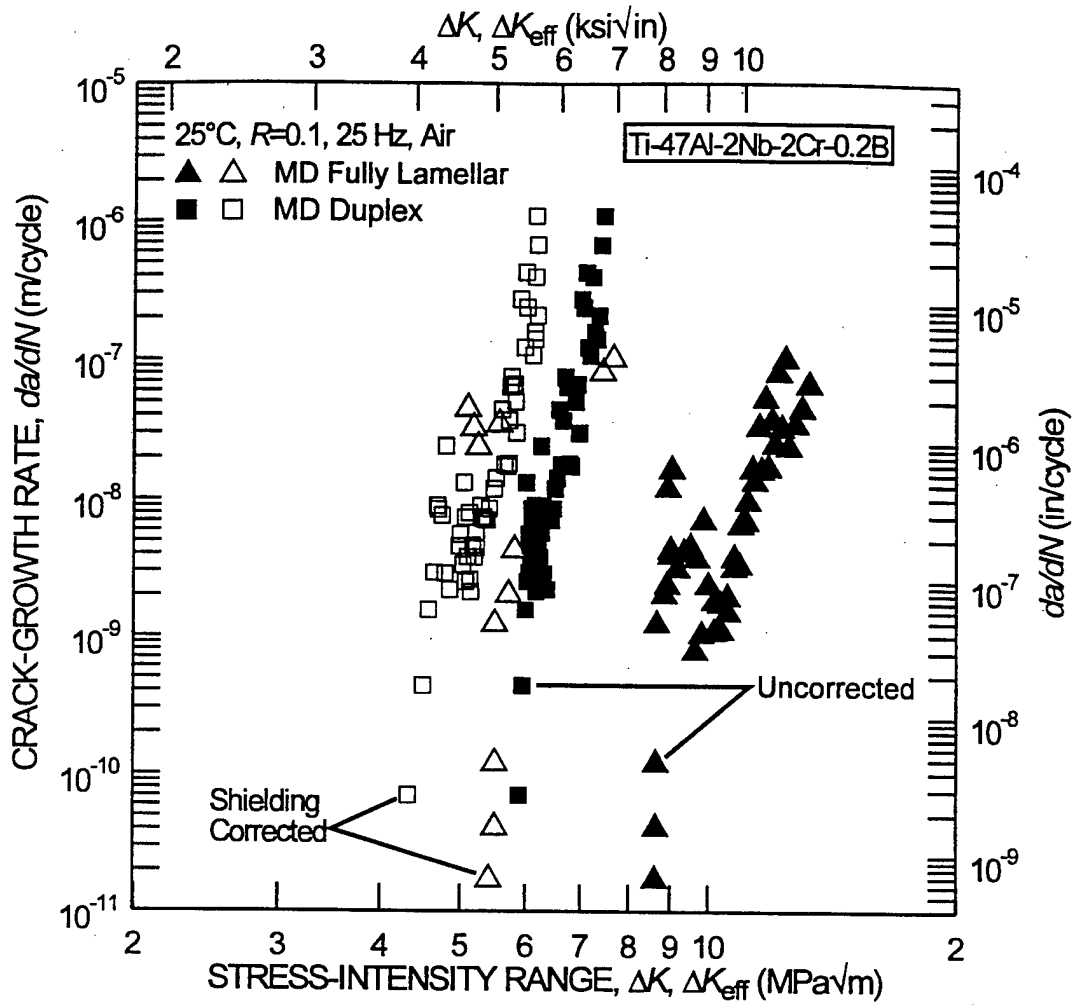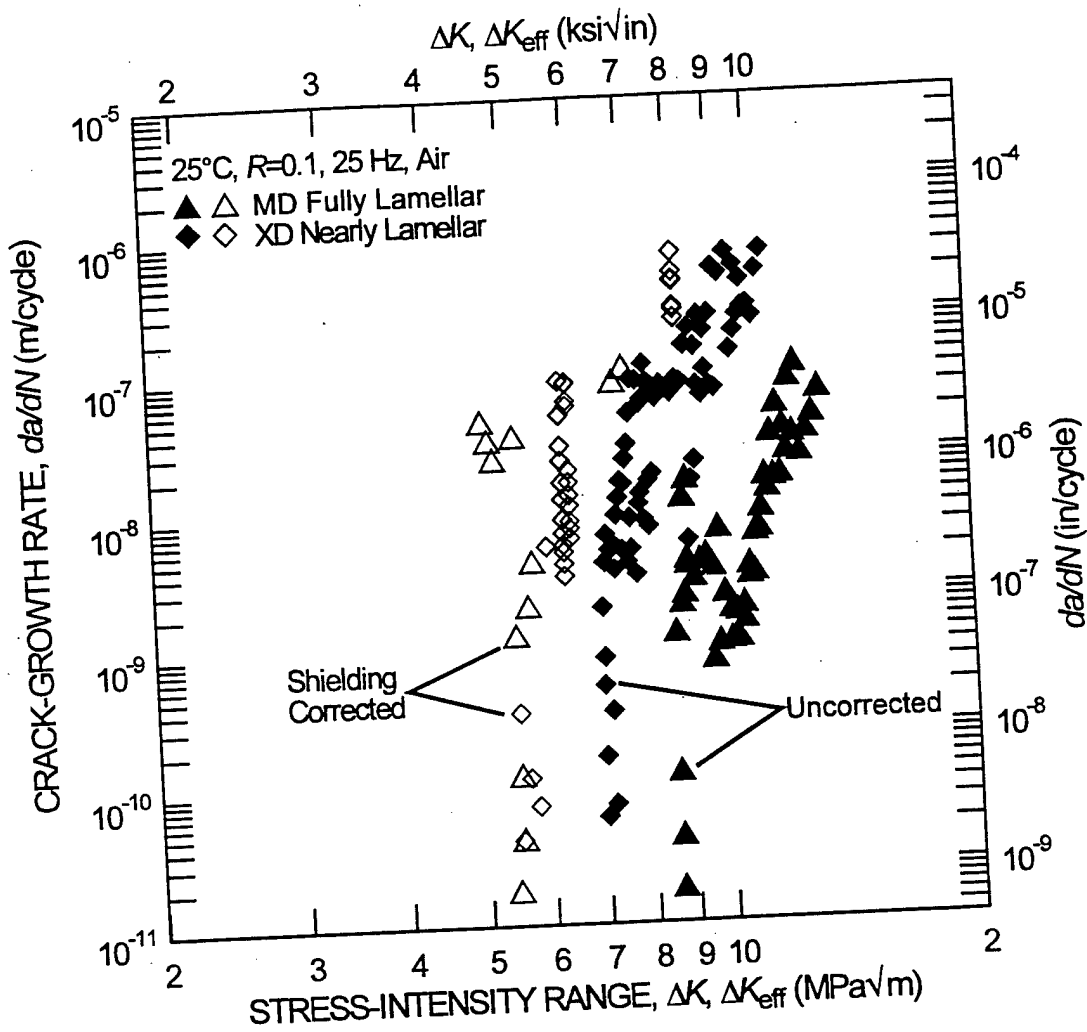
Fig. 1.8: Fatigue-crack growth rates, *da/dN*, for long cracks in the MD fully lamellar and XD nearly lamellar microstructures are plotted as a function of the applied stress intensity range, ΔK, and an effective, near-tip stress intensity range, ΔK_{eff}, from which the effect of extrinsic crack shielding mechanisms (closure and bridging) have been "subtracted". The normalization of growth rates by ΔK_{eff} indicates that the range of fatigue-crack growth resistance observed for the various lamellar microstructures can be largely attributed to variations in the degree of crack shielding provided by crack closure and uncracked ligament bridging.

2. ON THE ANOMALOUS TEMPERATURE DEPENDENCE OF FATIGUE-CRACK GROWTH IN γ-BASED TITANIUM ALUMINIDES

(A. L. McKelvey, K. T. Venkateswara Rao, and R. O. Ritchie)

2.1 Introduction

Recently, there has been considerable interest in γ-based titanium aluminides as light-weight structural materials, particularly in the aerospace industry where they are under consideration for gas-turbine engine applications. As they are candidate materials for elevated temperature use, an understanding of their fatigue and fracture properties at temperatures comparable to operating conditions is essential. In this regard, an anomalous temperature dependence of fatigue-crack propagation properties and the fatigue threshold (ΔK_{TH}) has been reported for γ-based alloys between ambient temperature and 800-850°C in air environments [1-3]. Although near-threshold growth rates are lower at 800°C than at 25°C, growth rates are higher at 600°C than at 25°C; similarly, thresholds are highest at 800°C and lowest at 600°C, with room temperature behavior in between. Based on observations that the effect is less striking *in vacuo* compared to air, as shown for a Ti-46.5Al-2Cr-3Nb-0.2W (K5) alloy with a fully lamellar microstructure in Fig. 2.1, Larsen *et al.* [1,4] attributed such behavior to environmental embrittlement and a lack of ductility at intermediate temperatures (on the assumption that ΔK_{TH} should increase with increasing temperature in the absence of embrittlement). Since this latter assumption is questionable, we consider here the role of crack-surface oxidation and its tendency to retard crack-growth rates, particularly at near-threshold levels, via crack-tip blunting and shielding by oxide-induced crack closure. In this study, the role of this mechanism on fatigue-crack growth rates in γ-based titanium aluminides is evaluated as a function of temperature, and an alternative explanation is presented for the anomalous temperature dependence of the near-threshold fatigue behavior.

2.2 Experimental Methods

The intermetallic material studied was a Ti-47.4Al-1.9Nb-0.9Mn (at.%) alloy containing ~1 vol.% TiB_2 particles fabricated through a proprietary XD^{TM} process [5]. The alloy was permanent mold cast into 40 mm diameter rods and subsequently hot-isostatic pressed at 1260°C and 172 MPa for 4 hours. The resulting microstructure consisted of fine lamellar (γ+α$_2$) colonies, ~120 μm in size, with ~30 vol.% of equiaxed γ grains, of average diameter ~23 μm, present along lamellar colony boundaries (Fig. 2.2).

18

The TiB$_2$ phase was present in the form of blocky particles, ranging between 1 - 5 μm in size, and needle shaped particles, ~20 - 50 μm long and 3 - 5 μm in diameter.

Fatigue-crack propagation tests were conducted using disk-shaped compact-tension DC(T) specimens (27 mm wide by 5 mm thick), which were cycled in air on an MTS servo-hydraulic testing machine at 600° and 800°C, i.e., below and above the ductile-to-brittle transition temperature (DBTT) for γ-TiAl, which has been reported to be ~700°C [6]. Fatigue tests were performed at 10 Hz (sine wave) under automated stress-intensity (K) control, in general accordance with the procedures described in ASTM Standard E647. Crack-propagation rates were measured as a function of the applied stress intensities, $\Delta K = K_{max} - K_{min}$, at constant positive load ratio of $R = 0.1$, defined as the ratio of the minimum to maximum stress intensities in the loading cycle ($R = K_{min}/K_{max}$). Load shedding schemes, with a K-gradient (the change in stress intensity per unit crack extension) ranging from -0.1 through -0.07 mm^{-1}, were used to approach the fatigue thresholds, ΔK_{TH} and $K_{max,TH}$, which were defined respectively as the ΔK and K_{max} values at which growth rates did not exceed ~10^{-10} m/cycle. Crack lengths were continuously monitored during cyclic loading using load-line based compliance methods; values were periodically verified *in situ* using optical measurements. Optical crack length measurements at elevated temperatures were made through a sapphire window furnace port using a high-resolution telescope equipped with a video camera. Good agreement, to within ± 200 μm, was obtained between compliance and telescopic measurements for crack length. Corresponding results at 25°C for the same alloy are included for comparison [7].

An attempt was made to directly measure the extent of crack closure [8] by estimating the closure stress intensity, K_{cl}, corresponding to the load where first deviation from linearity occurred with respect to displacement on unloading. Where closure occurs, an effective (near-tip) stress-intensity range, $\Delta K_{eff} = K_{max} - K_{cl}$, can be defined when $K_{cl} \geq K_{min}$. However, as the remoteness of measurement at elevated temperatures made a precise definition difficult, estimates for K_{cl} were instead calculated based on oxide thickness measurements. Auger spectroscopy in combination with focused-ion beam sputtering were used to measure the total oxide thickness on the fracture surfaces after final fracture. A calibration for the sputtering rate for this alloy was made by using a profilometer and a tantalum-oxide film with known thickness in conjunction with the spectroscopy. X-ray diffractometry, at grazing incident angles of 1°, 5° and 35°, was used to determine the constituents of the oxide films. At 800°C where the oxide scales were of micrometer dimensions, measurements were made on nickel-plated

19

metallographic sections, machined perpendicular to the fracture surfaces of fatigue cracks arrested at ΔK_{TH}.

2.3 Results and Discussion

Rates of fatigue-crack propagation in the fine lamellar microstructure at 25°, 600° and 800°C in air are shown in Fig. 3 for load ratios of 0.1 and 0.5. It is apparent that the fastest near-threshold growth rates ($<10^{-7}$ m/cycle) and lowest ΔK_{TH} values were measured at 600°C, just below the DBTT for TiAl, whereas the slowest near-threshold growth rates and highest thresholds were observed above the DBTT at 800°C; behavior at room temperature was intermediate. As noted above, this anomalous variation in fatigue-crack growth rates with temperature is a characteristic of many γ-TiAl alloys [1-3]. It is known that this phenomenon is effectively suppressed for crack growth *in vacuo* [1,4]; the present study further indicates that it is more pronounced at $R = 0.5$ compared to 0.1 and is absent at higher growth rates above -5×10^{-8} m/cycle (Fig. 2.3).

An explanation for this effect proposed by Larsen *et al.* [1,4] is that since ΔK_{TH} thresholds would normally increase with increasing temperature (in the absence of environmental effects), the data at 600-650°C are "anomalous" due to some unspecified environmental embrittlement at the lower temperature. In addition, it has been suggested that the effect is related to the increase in ductility above the DBTT at 800°C [2,3]. However, most models for intrinsic fatigue-crack growth imply that growth rates should increase, and ΔK_{TH} thresholds should *decrease*, with temperature (e.g., the simple crack-tip opening displacement model [9] where growth rates are inversely proportional to the yield strength and modulus). Accordingly, a much more probable explanation is that the 800°C data are "anomalous", particularly since the experimental data *in vacuo* for the K5 TiAl alloy (Fig. 2.1) confirm that indeed, without prominent environmental effects, thresholds decrease with temperature.

To explain any anomaly in the 800°C data, we note that the effect is most prevalent at near-threshold levels, which suggests a prominent role of crack closure; moreover, since high-temperature air environments are involved, a likely candidate is closure induced by oxidation products [10]. Indeed, the effect of such oxide-induced crack closure (OICC) on fatigue-crack growth in a duplex TiAl microstructure has been investigated as a function of load ratio by Soboyejo *et al.* [11], although temperature effects were not examined. Consequently, to evaluate the specific influence of OICC at the temperatures in question, Auger spectroscopy was used in combination with sputtering techniques and metallography to measure the peak thickness of the oxide

deposits on the fatigue fracture surfaces as a function of temperature and load ratio. Table 1 shows the oxide thickness measurements at the fatigue threshold.

Table 2.1

Total thickness of oxide deposits on fatigue surfaces at ΔK_{TH} at 25°, 600° and 800°C in air.

	25°C	600°C	800°C
$R = 0.1$	17 ± 10 nm	230 ± 12 nm	726 ± 81 nm
$R = 0.5$	22 ± 8 nm	120 ± 10 nm	266 ± 11 nm

Since OICC, in the form of premature contact of the crack surfaces on unloading, may be considered to be active when the peak oxide thickness is comparable with the minimum crack-tip opening displacement ($CTOD_{min}$) in the loading cycle, these data strongly suggest that closure is significantly more active at 800°C than at room temperature and 600°C. However, it is the *excess* oxide volume, i.e., the excess material inside the crack allowing for the conversion of metal, that is important in this comparison [12]. To compute these values, it is necessary to know the prevailing oxidation reaction(s).

Using X-ray diffractometry to identify the oxide constituents, it was found that TiO_2 followed by Al_2O_3 exhibited the strongest characteristic X-ray peaks at both 600° and 800°C, indicating that TiO_2 and Al_2O_3 occupy the largest mole fraction of the oxide layer; smaller amounts of TiN, Ti_3AlN, pure Ti and MnO_2 were also detected. Accordingly, to determine the thickness of excess material on the fracture surfaces, the volume ratio of oxide to metal of an oxidation reaction, i.e., the Pilling-Bedworth (P-B) ratio [13], was determined. To simplify the analysis, the following reactions which only consider the formation of TiO_2 and Al_2O_3, were used to approximate the actual P-B ratio, since these reaction products make up the largest mole fraction of actual corrosion products formed:

$$Ti_3Al + 2O_2 \rightarrow 2TiO_2 + TiAl$$
$$2Ti_3Al + 15/2O_2 \rightarrow 6TiO_2 + Al_2O_3$$
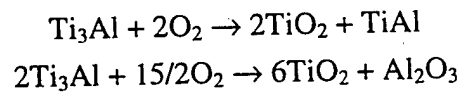
These reactions represent upper and lower bounds for the P-B ratios, which have values of 1.56 and 1.14 respectively. Since the oxide layer may have resulted from several reactions simultaneously, the bulk P-B ratio was taken as the average value of 1.32 in

order to calculate excess oxide thicknesses; these are listed in Table 2.2, together with corresponding $CTOD_{min}$ values at the threshold.

Table 2.2

Comparison of estimated $CTOD_{min}$ at ΔK_{TH} and excess oxide thickness at 25°, 600° and 800°C.

	25°C		600°C		800°C	
	$CTOD_{min}$ nm	excess oxide thickness, d nm	$CTOD_{min}$ nm	excess oxide thickness, d nm	$CTOD_{min}$ nm	excess oxide thickness, d nm
$R = 0.1$	2.5	13	4	175	11	552
$R = 0.5$	154	17	170	91	430	202

Table 2.2 gives a clear indication of the relative effects of OICC over the temperature range in question through a comparison of the excess oxide thickness, d, with the $CTOD_{min}$; moreover, further insight can be gained by estimating the closure stress intensities, K_{cl}, by assuming that the oxide is a rigid wedge inside the crack [12], viz:

$$K_{cl} = \frac{Ed}{4\sqrt{\pi l}\left(1 - v^2\right)} \tag{1}$$

where d is the peak excess oxide thickness, $2l$ is its location behind the tip, $E/(1-v^2)$ is the effective Young's modulus in plane strain, and v is Poisson's ratio. From Eq. 1, values of K_{cl} at 25° and 600°C were estimated, respectively, to be 0.3 and 3.1 MPa√m at a load ratio of 0.1 and ~0.3 and 1.6 MPa√m at R = 0.5. At 800°C, K_{cl} values were considerably greater with corresponding estimates being, respectively, 9.8 and 3.6 MPa√m at load ratios of 0.1 and 0.5

From these considerations and Table 2.2, it is apparent that the role of OICC at 25°C is small (e.g., $K_{cl} < K_{min}$ at low R); indeed it is essentially negligible at $R = 0.5$ where $d << CTOD_{min}$. At 600°C, the role of OICC is still relatively minor, as $d < CTOD_{min}$ at $R = 0.5$; even at $R = 0.1$, K_{cl} values are still only a small fraction of the $K_{max,TH}$ threshold, i.e., $K_{cl}/K_{max,TH} < 0.39$. However, at 800°C, the extent of crack-surface oxidation is extensive, $d >> CTOD_{min}$ at $R = 0.1$, such that the reduction in the near-tip driving force for crack extension due to oxide wedging is substantial (i.e., $K_{cl}/K_{max} \sim 0.77$ at ΔK_{TH}).

Since fatigue-crack propagation can be considered as the mutual competition of intrinsic microstructural damage mechanisms ahead of the crack tip, which *promote* crack advance, and extrinsic crack-tip shielding (e.g., closure) mechanisms, behind the tip, which act to *impede* it [15], we conclude that the anomalous temperature effect on the near-threshold fatigue of γ-TiAl base alloys results directly from this interplay. Indeed, if the crack-growth rates in Fig. 2.3 are re-plotted as a function of ΔK_{eff} after "correcting" for such closure (Fig. 2.4), the anomalous temperature dependence disappears. Rather than growth rates being accelerated (and ΔK_{TH} thresholds lowered) at intermediate temperatures due to some unspecified environmental embrittlement and a lack of ductility below the DBTT [2], it is proposed that as the intrinsic fatigue resistance decreases with increasing temperature (as shown by the *in vacuo* data), growth rates are instead retarded (and ΔK_{TH} thresholds increased) at 800°C due to the substantial effect of crack closure from the wedging of crack-surface oxidation products. This explanation is consistent with the *in vacuo* results (Fig. 2.1), all oxidation data (Table 2.2), and simple intrinsic models for fatigue-crack growth [9]; moreover, the sudden onset of threshold behavior at high growth rates, shown by the 800°C data (Fig. 2.3), is very characteristic of the cessation of crack growth due to thermal oxide wedging (e.g., [16]).

2.4 Conclusions

Based on a study of the fatigue-crack growth behavior at $R = 0.1$ and 0.5 between 25° and 800°C in a γ-TiAl based XD™ Ti-47.4Al-1.9Nb-0.9Mn (at.%) titanium aluminide alloy (containing ~1 vol.% TiB_2 particles), with a fine (~120 μm sized) lamellar microstructure, the following conclusions can be made:

1. An anomalous temperature effect on fatigue-crack propagation rates is confirmed in that growth rates are found to be lower at 800°C than at 25°C yet are higher at 600°C than at 25°C; similarly ΔK_{TH} thresholds are highest at 800°C and lowest at 600°C, with room temperature behavior in between. The effect, however, is only seen in air environments and predominates at near-threshold levels below ~5 × 10^{-8} m/cycle.

2. Rather than being associated with some unspecified embrittlement at 600°C, the effect is ascribed to a dominant role of oxide-induced crack closure at 800°C, which retards near-threshold crack growth rates and results in a premature arrest of crack growth at a higher ΔK_{TH} threshold value. This explanation is consistent with results *in vacuo*, measurements of crack-surface oxidation debris, and simple intrinsic models for fatigue-crack growth.

2.5 References

1. S. J. Balsone, J. M. Larsen, D .C. Maxwell and J. W. Jones, *Mater. Sci. Eng. A* **192/193**, 457 (1995).

2. J. M. Larsen, B. D. Worth, S. J. Balsone and J. W. Jones, in *Gamma Titanium Aluminides*, eds. Y.-W. Kim, R. Wagner and M. Yamaguchi, p. 821, TMS, Warrendale, PA (1995).

3. K. T. Venkateswara Rao, Y.-W. Kim and R. O. Ritchie, *Scripta Metall. Mater.* **33**, 459 (1995).

4. J. M. Larsen and S. J. Balsone, *personal communication*, Dec. 1995.

5. D. E. Larsen and M. Behrendt, in *Fatigue and Fracture of Ordered Intermetallic Materials: I*, eds. W. O. Soboyejo, T. S. Srivatsan and D. L. Davidson, p. 27, TMS, Warrendale, PA (1994).

6. H. A. Lipsitt, D. Schectman and R. E. Schafrik, *Metall. Trans. A* **6**, 1991 (1975).

7. J. P. Campbell, K. T. Venkateswara Rao and R. O. Ritchie, in *Fatigue '96*, eds. G. Lütjering and H. Nowack, Sixth International Conference on Fatigue, Berlin, Germany, p. 1779, Pergamon, Oxford, UK (1996).

8. W. Elber, *Eng. Fract. Mech.* **2**, 37 (1970).

9. F. A. McClintock, in *Fatigue Crack Propagation*, ASTM STP 415, p. 170, Amer. Soc. Test. Matls., Philadelphia, PA (1967).

10. S. Suresh, G. F. Zamiski and R. O. Ritchie, *Metall. Trans. A* **12**, 1435 (1981).

11. W. O. Soboyejo, J. E. Deffeyes and P. B. Aswath, *Mater. Sci. Eng. A* **138**, 95 (1991).

12. S. Suresh and R. O. Ritchie, *Eng. Fract. Mech.* **18**, 785 (1983).

13. O. Kubaschewski and B. E. Hopkins, *Oxidation of Metals and Alloys*, Academic Press, New York, NY (1953).

14. S. Suresh and R. O. Ritchie, in *Fatigue Crack Growth Threshold Concepts*, eds. D. L. Davidson and S. Suresh, p. 227, TMS, Warendale, PA, (1984).

15. R. O. Ritchie, *Mater. Sci. Eng. A* **103**, 15 (1988).

16. J. L. Yuen, P. Roy and W. D. Nix, *Metall. Trans. A* **15**, 1769 (1984).
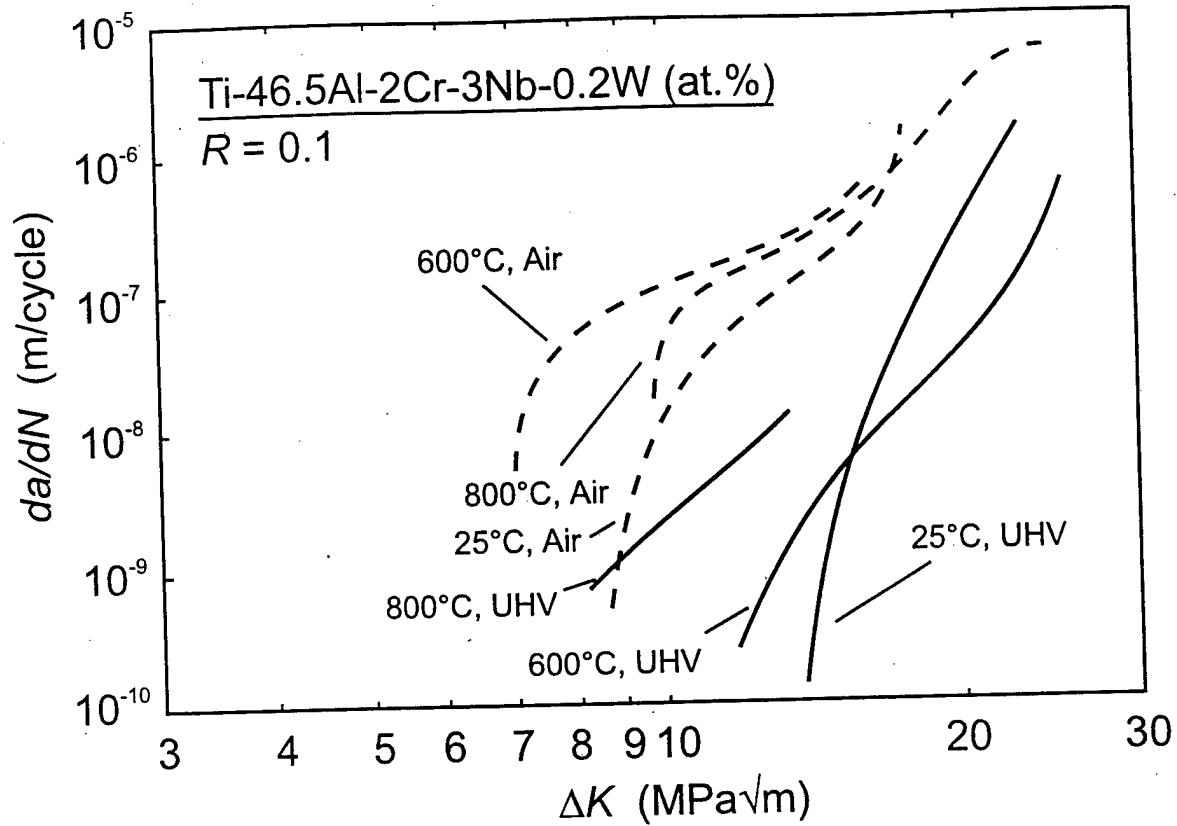
Fig. 2.1: Variation of fatigue-crack propagation rates, da/dN, as a function of the stress-intensity range, ΔK, in the K5 (Ti-46.5Al-2Cr-3Nb-0.2W) alloy at $R = 0.1$ at $25°$, $600°$ and $800°C$ in room air and an ultrahigh vacuum (UHV) of ~6×10^{-7} Pa (after Larsen *et al.* [1,4]).

Fig. 2.2: Optical micrograph of the microstructure of the XD™-processed Ti-47.4Al-1.9Nb-0.9Mn (at.%) alloy containing ~1 vol.% TiB_2 particles, heat treated to a fine lamellar ($\gamma+\alpha_2$) microstructure with ~30 vol.% equiaxed γ grains along lamellar colony boundaries (etchant: 2% HF, 5% H_3PO_4).
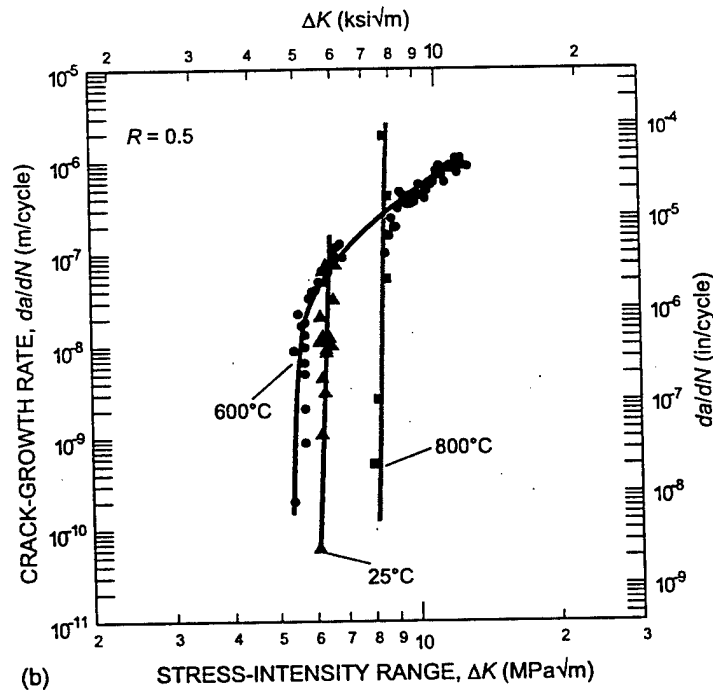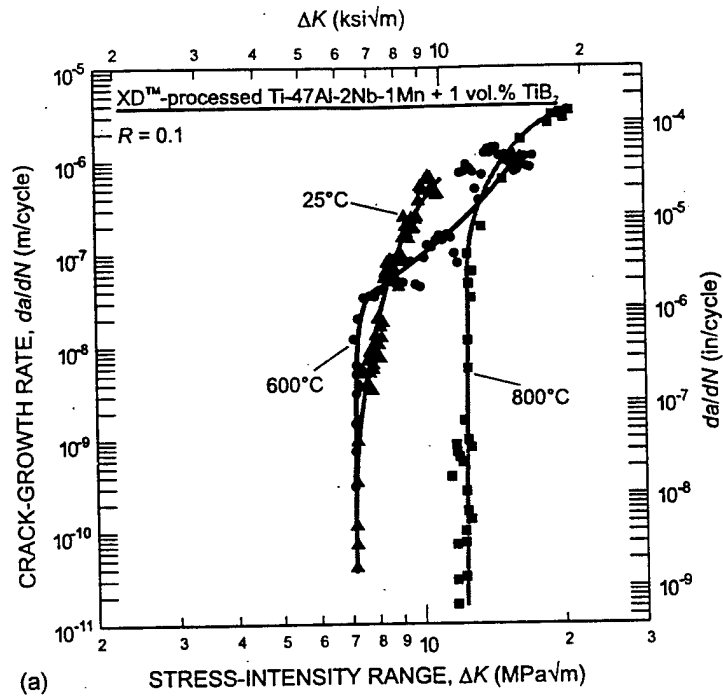
Fig. 2.3: Variation of fatigue-crack propagation rates, da/dN, with temperature ($25°$, $600°$ and $800°C$) at (a) $R = 0.1$ and (b) $R = 0.5$ in the XD™-processed Ti-47.4Al-1.9Nb-0.9Mn (at.%) alloy containing ~1 vol.% TiB$_2$ particles. Note how the fatigue thresholds are lowest at $600°C$ and highest at $800°C$, with $25°C$ data in between.

Fig. 2.4: Variation of fatigue-crack propagation rates, *da/dN*, at $R = 0.1$ with the effective stress-intensity range ($\Delta K_{eff} = K_{max} - K_{cl}$) in the XD™-processed Ti-47.4Al-1.9Nb-0.9Mn (at.%) alloy containing ~1 vol.% TiB₂. Note how after "correcting" for crack closure, the "anomalous temperature effect" on fatigue thresholds disappears.

27

3. ON THE GROWTH OF SMALL FATIGUE CRACKS IN γ-BASED TITANIUM ALUMINIDES

(J. P. Campbell, J. J. Kruzic, S. Lillibridge, K. T. Venkateswara Rao and R. O. Ritchie)

3.1 Introduction

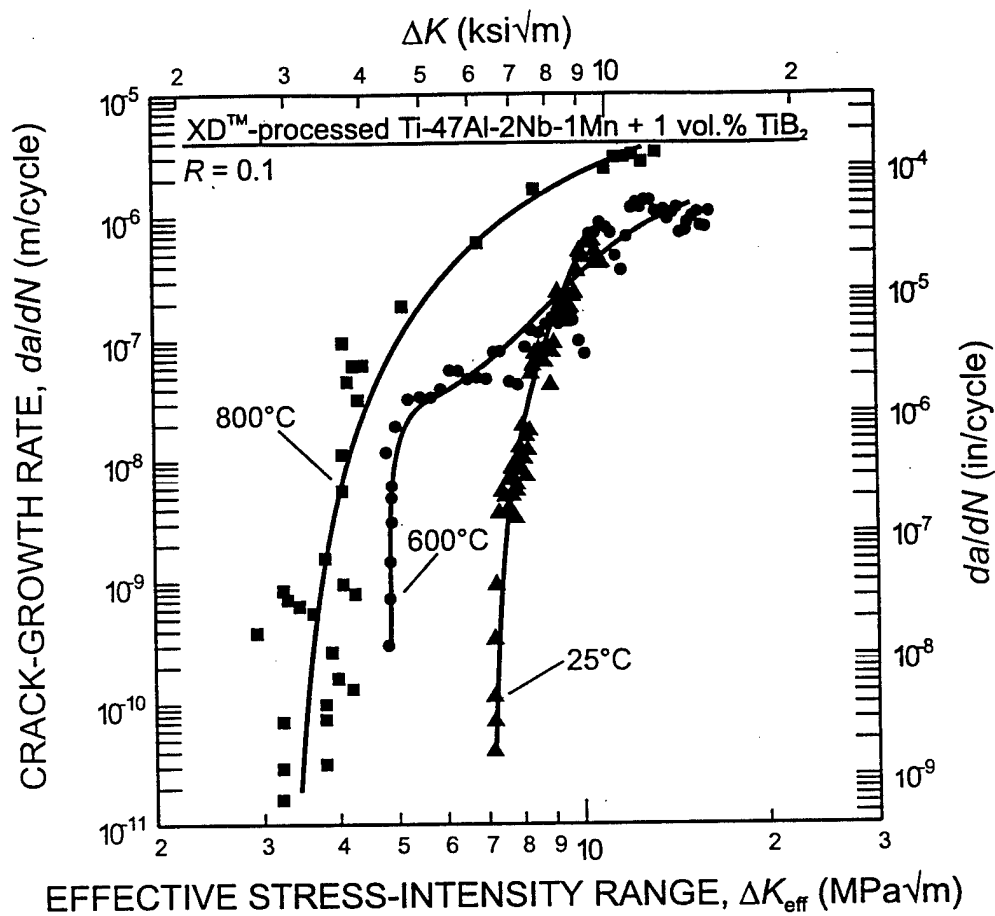Gamma-based TiAl intermetallic alloys have received considerable attention recently as candidate materials for high-temperature aerospace applications [1-4]. Two classes of microstructure have been prominent in the two-phase ($\gamma + \alpha_2$) alloys: a lamellar structure consisting of lamellar colonies containing alternating γ and α_2 platelets, and a duplex structure consisting of equiaxed grains of γ with small amounts of α_2 grains [1]. In general, duplex structures display better elongation and strength, whereas lamellar structures show better toughness and fatigue crack-growth resistance [2,5-8]. However, a problem with both microstructures, as with most intermetallics, is that fatigue-crack growth rates, da/dN, show a very strong dependence upon the applied stress-intensity range, ΔK, i.e., $da/dN \propto \Delta K^m$, where m is greater than ~10 [11,12]. With such high exponents, predicted component lives based on damage-tolerant analyses are often unacceptably sensitive to applied stress levels, necessitating that the applied ΔK levels remain below a fatigue threshold, ΔK_{TH}. In the presence of "small cracks", however, this approach may be non-conservative.

Small cracks (typically < ~500 μm in length) are known to grow at applied ΔK below the "long crack" threshold, and to exhibit growth rates in excess of those corresponding to long cracks (typically larger than 2-3 mm) at the same *applied* ΔK levels [11-14]. Such effects are apparent when crack sizes become comparable to i) the characteristic microstructural dimensions (a continuum limitation), ii) the extent of local inelasticity (i.e., the plastic-zone size) *ahead* of the crack tip (a linear-elastic fracture mechanics limitation), or iii) the extent of the zone of crack-tip shielding *behind* the crack tip (a similitude limitation). Accordingly, the objective of the present study is to examine the small-crack effect in a commercial γ-based TiAl alloy by comparing the growth-rate behavior of long (through-thickness) cracks with that of small surface cracks for both duplex and fully lamellar microstructures.

3.2 Materials and Experimental Procedures

The TiAl alloy studied, of nominal composition (at.%) Ti-47Al-2Nb-2Cr-0.2B, contained B additions which resulted in ~0.5 vol.% of needle-like TiB$_2$ particles (~2-10

28

μm in length and ~1 μm in diameter). The lamellar microstructure was obtained by a two-step forging process, followed by heat treating in flowing argon gas at 1370°C for 1 hr, air cooling and then holding 6 hr at 900°C prior to argon gas furnace cooling. The resulting microstructure featured ~145 μm-sized lamellar colonies with very small amounts (~4%) of fine equiaxed γ grains (5-20 μm) between lamellar colonies; the α_2 layer (center-to-center) spacing was ~1.3 μm (Fig. 3.1a). The duplex microstructure was achieved through a furnace cool after heat treating the forged alloy at 1320°C for 3 hr in argon. The structure consisted of nearly equiaxed grains of the γ-phase, ~17 μm in diameter (Fig. 3.1b), with ~10 vol.% α_2 present in the form of thin layers (~1-3 μm thick) at grain boundaries or as larger "blocky" regions (~3-23 μm in diameter) at triple points. A small proportion of fine lamellar colonies was also present.

Long (> 5 mm) crack growth rates were measured on through-thickness cracks using 4-mm thick compact-tension, C(T), specimens. Tests were conducted in 25°C air at 25 Hz (sine wave) in accordance with ASTM Standard E647; a load ratio, R, of 0.1 (= K_{min}/K_{max}) was maintained. Fatigue thresholds, ΔK_{TH}, operationally defined as the applied ΔK below which $da/dN < 10^{-10}$ m/cycle, were approached using a variable-ΔK/constant-R load-shedding scheme. Crack lengths were monitored using electrical-potential measurements (on NiCr foil gauges bonded to the side face of the specimen) and using back-face strain compliance.

Elastic compliance data were also utilized to measure the extent of crack-tip shielding from crack closure and crack bridging. Crack closure was evaluated in terms of the closure stress intensity, K_{cl}, which was approximately defined at the load corresponding to first deviation from linearity on the unloading compliance curve [15,16]. Crack bridging was assessed through a comparison of the experimentally measured unloading compliance (at loads above those associated with closure) with the theoretical value for a traction-free crack [17]. With this technique, a bridging stress intensity, K_{br}, representing the reduction in K_{max} due to the bridging tractions developed in the crack wake, was estimated.

Small ($c < 300$ μm) crack growth rates were investigated using unnotched rectangular beams (of width 10 mm, thickness 6 mm, and span 50 mm), loaded in four-point bending. Small surface cracks associated with electro-discharge machining (EDM) pit damage were cyclically loaded to grow the cracks away from the EDM heat-affected zone (HAZ) prior to data acquisition (HAZ was identified optically using an aqueous 2% HF, 5% H_3PO_4 etchant on a polished surface). In some instances, sample surfaces were ground and polished following pitting to completely eliminate the HAZ, leaving only

small cracks on the surface. Using this procedure, initial surface flaws with half lengths less than $c \sim 125$ μm were achieved.

Bend samples were cycled at $R = 0.1$ between 5 and 25 Hz (sine wave), with crack lengths monitored by periodic surface replication using cellulose acetate tape. Replicas were Au or Pt coated to improve resolution prior to optical measurement of crack lengths. Average growth rates were computed from the amount of crack extension between two discrete measurements. Stress intensities were determined using linear-elastic solutions for surface cracks in bending [18], assuming a semi-circular crack profile (crack depth to half surface crack length ratio, $a/c = 1$). This assumption was verified by heat tinting select samples at 600°C for 4 hr prior to fracture to measure the crack shape; measurements revealed an average a/c ratio of 1.04 which corresponds to a semi-circular crack.

3.3   Results and Discussion

Figure 3.2 shows the fatigue-crack growth rates of through-thickness long cracks in the lamellar and duplex microstructures. Growth rates are clearly a strong function of ΔK, with Paris power-law exponents, m, in the mid-growth-rate regime ranging from 9 in the lamellar to 22 in the duplex structure. Crack-growth resistance is considerably greater in the lamellar structure; indeed growth rates (at a specific ΔK) are up to five orders of magnitude lower and threshold ΔK_{TH} values $\sim 1\frac{1}{2}$ times larger than in the duplex material, resulting from a significant role of crack-tip shielding [4,8,19].   Under monotonic loading, inter- and intra-lamellar microcracking ahead of the crack tip results in the development of uncracked ("shear") ligament bridges in the crack wake [20,21]. Crack bridging by these ligaments is the principal mechanism of toughening in the lamellar microstructure [20], with a bridging stress intensity K_{br} on the order of 12 MPa√m [19]. No such bridging is seen in the duplex material. Under cyclic loading in the lamellar structure, the bridging is diminished in part due to fatigue failure of the ligaments; nevertheless, it still has a prominent effect [19], i.e., K_{br} values in fatigue have been measured as high as 2 MPa√m (14% of K_{max}) at $\Delta K \sim 13$ MPa√m. In addition, the resulting meandering crack paths promote (roughness-induced) crack closure from the wedging of asperities [19]. Although the interpretation of closure measurements can be somewhat uncertain in the presence of bridging, measured K_{cl} values at $R = 0.1$ ranged from ~ 4-7 MPa√m in the lamellar structure to ~ 1.6-2.2 MPa√m in the duplex structure.

Corresponding results for the growth of cracks with half surface lengths between ~ 35-275 μm are plotted in Fig. 3.2. Clearly, small-crack growth rates have

characteristically far greater scatter than long-crack data, associated with a biased sampling of the microstructure by flaws which are comparable in size with microstructural dimensions [22]. Moreover, in marked contrast to long-crack behavior, the scatter bands for the lamellar and duplex microstructures essentially overlap, although crack growth in the lamellar structure occurs at slightly lower ΔK levels. The most significant results, however, are that, at equivalent applied ΔK levels, small-crack growth rates exceed those of corresponding long cracks by up to 3 orders of magnitude, and crack growth is observed in both structures at applied ΔK levels well below the long-crack threshold, ΔK_{TH}. Specifically, small-crack growth is evident at applied ΔK levels as low as 3.5 and 4.7 MPa√m in the lamellar and duplex structures, respectively; corresponding long-crack thresholds are, respectively, 8.6 and 6.0 MPa√m. Differences between long- and small-crack behavior, however, are much reduced in the duplex microstructure.

Given the salient role of shielding in the crack-growth resistance of γ-based TiAl alloys, in particular for the lamellar microstructure, it is likely that small flaws in these alloys will be susceptible to a *similitude limitation*. In other words, by virtue of their limited wake, they do not develop equilibrium zones of crack-tip shielding akin to long cracks. Such shielding, which arises primarily from uncracked ligament bridging and roughness-induced crack closure, is much less prominent in the duplex structure, consistent with the minimal difference in small- and long-crack data in this microstructure. Indeed, since the superior long fatigue crack-growth properties of lamellar microstructures have been principally attributed to shielding mechanisms [19], the similar fatigue crack-growth properties of the duplex and lamellar structures for small-crack sizes would appear to result from a reduced shielding contribution at these crack sizes. The limited role of such shielding during small-crack growth and the observed similarity of the duplex and lamellar small-crack data thus implies that there is little difference in *intrinsic* fatigue crack-growth resistance of the two microstructures.

To verify this similitude limitation quantitatively, the shielding contributions from both uncracked ligament bridging and crack closure were experimentally measured and "subtracted" from the long crack results on the assumption that the effective (local) driving force at the crack tip, ΔK_{eff}, can be described (for $K_{cl} > K_{min}$) by:

$$\Delta K_{eff} = (K_{max} - K_{br}) - K_{cl} . \qquad (1)$$

Here K_{br} is the bridging stress intensity associated with bridging tractions developed across the crack flank, and K_{cl} is the closure stress intensity, arising primarily from the

wedging of fracture-surface asperities inside the crack. Specific measurements of K_{br} and K_{cl} are documented in ref. 19; results in terms of their effect on the normalization of long- and small-crack data are shown respectively in Figs. 3.3a and b for the lamellar and duplex microstructures.

As illustrated in Fig. 3.3, replotting the long-crack data in terms of ΔK_{eff} after correcting for bridging and closure results in a far closer correspondence between the long and small crack behavior, although the normalization is less effective for the lamellar microstructure where small-crack growth is evident at stress intensities below the $\Delta K_{TH,eff}$ threshold. This is, however, to be expected because crack sizes are comparable to the scale of the coarser lamellar microstructure (*continuum limitation*). For crack sizes smaller than the grain size, the crack front of the elliptical flaw at most sampled only a few lamellar colonies. Prior studies of the effect of lamellar orientation on fatigue crack-growth rates have indicated that growth rates are faster when cracking is coplanar with the lamellar (γ/α_2) interface, particularly at low ΔK levels [23-26]. It is thus unlikely that a continuum parameter such as the long-crack threshold, which is determined for a large crack which samples many lamellar colonies, would reflect the worst-case growth-rate behavior of a small crack confined to only one or two colonies.

In terms of the potential use of γ-TiAl alloys in fatigue-critical situations, the present data suggest a somewhat surprising result that the duplex microstructure may offer the better properties and be more amenable to reliable application in damage-tolerant design. Indeed, although the scatter bands for the two alloys largely overlap, the lamellar structure exhibits small-crack growth at lower ΔK levels. Moreover, as design may have to be based on a fatigue threshold due to the steep exponents in the (long) crack-growth law, the ability to define a lower-bound threshold value will be critical. The definition of such limits appears feasible for duplex microstructures in terms of (a shielding-corrected) $\Delta K_{TH,eff}$ threshold, at least for crack sizes larger than characteristic microstructural dimensions (~20 μm). In contrast, it is more difficult to define a similar threshold for the lamellar structures as characteristic microstructural dimensions are up to an order of magnitude larger. Accordingly, the growth rates of small fatigue cracks up to $c \sim 300$ μm in length show considerable scatter due to statistical sampling of the microstructure, and continue to propagate at stress intensities below the $\Delta K_{TH,eff}$ threshold.

3.4 Conclusions

Based on an experimental study of the fatigue-crack growth behavior of long (>5 mm) through-thickness and small ($c < 300$ μm) surface cracks in duplex and lamellar microstructures in a Ti-47Al-2Nb-2Cr-0.2B (at.%) alloy at 25°C, the following conclusions can be made:

1. Small-crack growth rates in both microstructures are faster than those of corresponding long cracks at the same applied ΔK levels; moreover, small cracks are found to propagate at applied ΔK levels below the long-crack threshold ΔK_{TH}.

2. This effect is primarily attributed to the role of crack-tip shielding, principally from uncracked ligament bridging and crack closure, in impeding long-crack growth rates (similitude limitation), as closer correspondence between long- and small-crack data is achieved after "correcting" for such shielding. Small-crack growth, however, is still evident below this lower-bound threshold in lamellar structures even after such normalization, due to statistical sampling of the coarser microstructure (continuum limitation).

3. A comparison of long-crack data suggest that the fatigue crack-growth resistance of the lamellar structure is significantly greater than that of the duplex structure, with growth rates being up to five orders of magnitude lower at equivalent ΔK levels. A comparison of small-crack data, conversely, indicates marginally superior fatigue crack-growth resistance in the duplex structure (although the scatter bands for the two structures overlap).

4. Duplex microstructures appear to offer better properties from the perspective of their potential use in fatigue-critical applications. In addition to their higher strength and ductility, the definition of a shielding-corrected (lower-bound) $\Delta K_{TH,eff}$ threshold, below which both small- and long-cracks are dormant, appears feasible. Such an approach is less certain for the coarser lamellar microstructures where small cracks of grain-size dimensions continue to propagate below this lower-bound threshold (a continuum limitation).

3.5 References

1. Y.-W. Kim, *J. Metals* **46:7**, 30 (1994).

2. Y.-W. Kim and D. M. Dimiduk, *J. Metals* **43:8**, 40 (1991).

3. G. F. Harrison and M. R. Winstone, in *Mechanical Behaviour of Materials at High Temperature*, eds. C. M. Branco, R. O. Ritchie and V. Sklenicvka, Kluwer, 309 (1996).

4. J. M. Larsen, B. D. Worth, S. J. Balsone and J. W. Jones, in *Gamma Titanium Aluminides*, eds. Y.-W. Kim *et al.*, TMS, Warrendale, PA, 821 (1995).

5. K. S. Chan, *Metall. Trans. A* **24**, 569 (1993).

6. K. S. Chan and Y.-W. Kim, *Metall. Trans. A* **23**, 1663 (1992).

7. K. S. Chan and Y.-W. Kim, *Metall. Trans. A* **24**, 113 (1993).

8. K. T. Venkateswara Rao, Y.-W. Kim, C. L. Muhlstein and R. O. Ritchie, *Mater. Sci. Eng.* **A192/193**, 474 (1995).

9. K.T. Venkateswara Rao, Y.-W.Kim, R. O. Ritchie, *Scripta Metall. Mat.* **33**, 495 (1995).

10. K. Badrinarayanan, A. L. McKelvey, K. T. Venkateswara Rao and R. O. Ritchie, *Metall. Mat. Trans. A* **27**, 3781 (1996).

11. K. J. Miller, *Fat. Eng. Mater. Struct.* **5**, 223 (1982).

12. J. Lankford, *Fat. Eng. Mater. Struct.* **8**, 161 (1985).

13. S. Suresh and R. O. Ritchie, *Int. Metals Rev.* **29**, 445 (1984).

14. R. O. Ritchie and J. Lankford, *Mater. Sci. Eng.* **A84**, 11 (1986).

15. W. Elber, *Eng. Fract. Mech.* **2**, 37 (1970).

16 R. O. Ritchie and W. Yu, in *Small Fatigue Cracks*, eds., R. O. Ritchie and J. Lankford, TMS, Warrendale, PA, 167 (1986).

17. R. O. Ritchie, W. Yu and R. J. Bucci, *Eng. Fract. Mech.* **32**, 361 (1989).

18. J. C. Newman, Jr. and I. S. Raju, *Eng. Fract. Mech.* **15**, 185 (1981).

19. J. P. Campbell and R. O. Ritchie, *Metall. Mat. Trans. A,* in review (1997); (available as J. P. Campbell, M.S. Thesis, University of California at Berkeley, 1996).

20. K. S. Chan, *Metall. Mat. Trans. A* **26**, 1407 (1995).

21. K. S. Chan, *Metall. Trans. A* **22**, 2021 (1991).

22. K. T. Venkateswara Rao, W. Yu and R. O. Ritchie, *Eng. Fract. Mech.* **31**, 623 (1988).

23. D. L. Davidson and J. B. Campbell, *Metall. Trans. A* **24**, 1555 (1993).

24. P. Bowen, R. A. Chave and A. W. James, *Mater. Sci. Eng. A* **A192/193**, 443 (1995).

25. D. J. Wissuchek, G. E. Lucas and A. G. Evans, in *Gamma Titanium Aluminides*, eds. Y.-W. Kim *et al.*, TMS. Warrendale, PA, 875 (1995).

26. R. Gnanamoorthy, Y. Mutoh, K. Hayashi and Y. Mizuhara, *Scripta Metall. Mat.* **33**, 907 (1995).
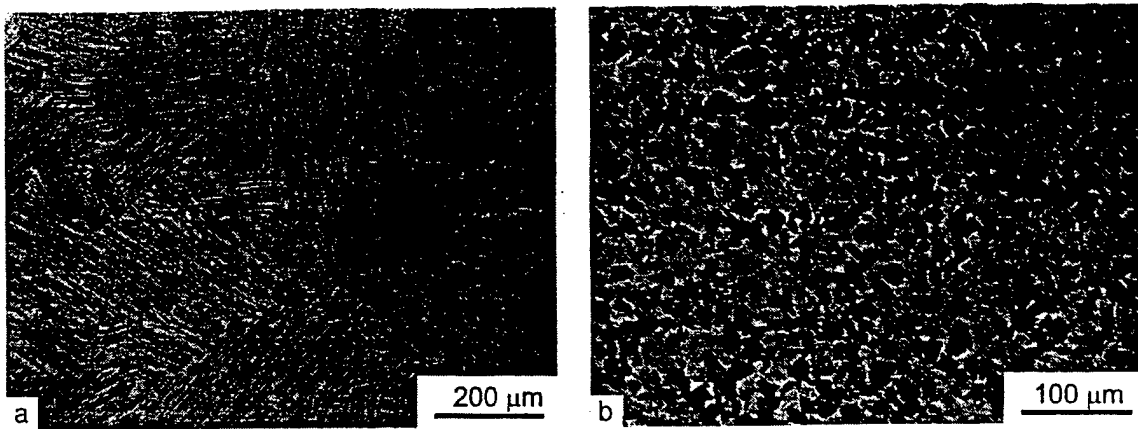
Fig. 3.1: Optical micrographs of the (a) lamellar and (b) duplex microstructures in Ti-47Al-2Nb-2Cr-0.2B (at.%). Etchant: aqueous 2% HF/ 5% H_3PO_4.

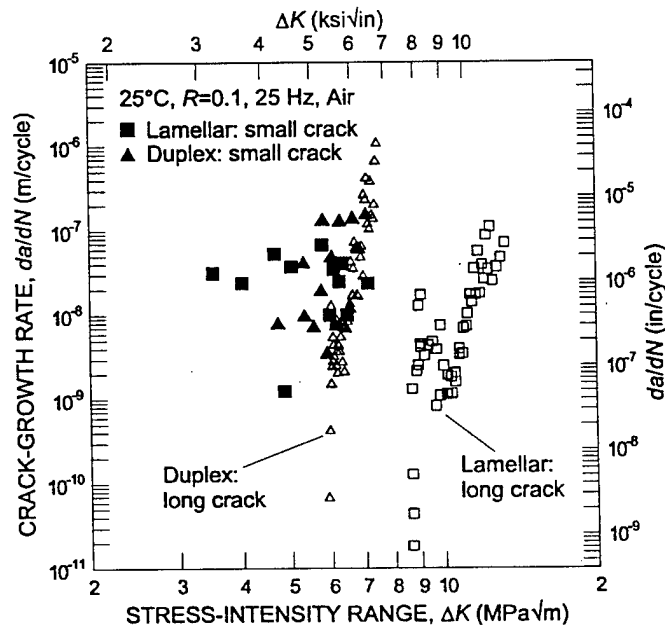Fig. 3.2: Fatigue crack-growth rates for through-thickness long cracks ($a > 5$ mm) and small surface cracks ($c \sim 35$-275 μm) in the lamellar and duplex microstructures of Ti-47Al-2Nb-2Cr-0.2B. Small-crack data points represent average growth rates over a specific increment of crack extension (between two surface replications).
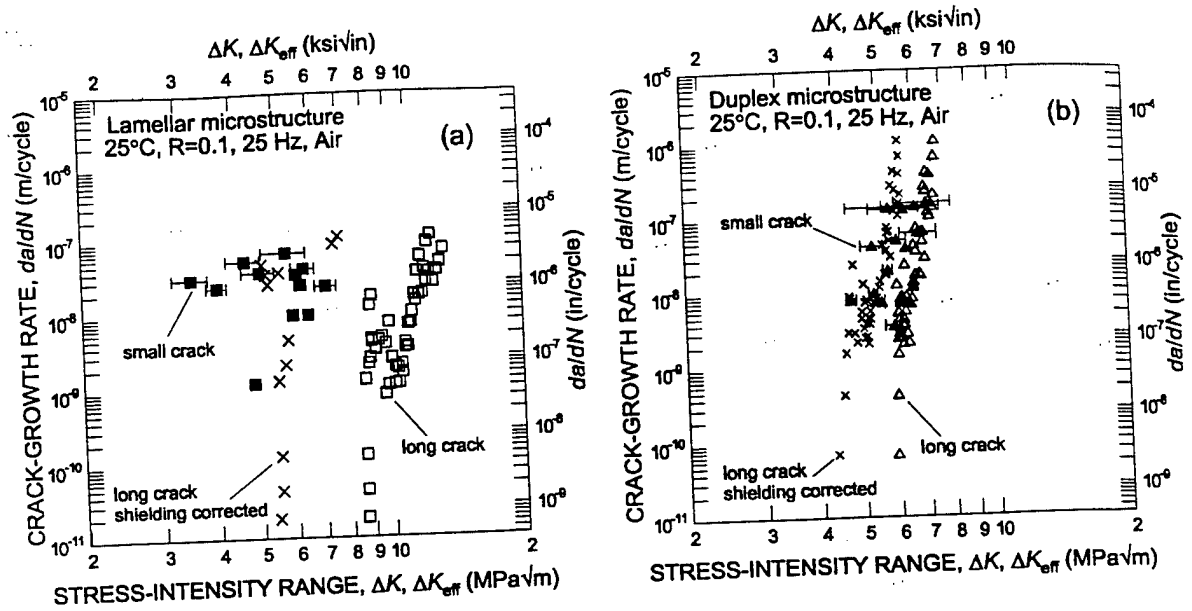
Fig. 3.3: Comparison of long-crack, small-crack, and shielding corrected long-crack fatigue data in the (a) lamellar and (b) duplex microstructures. Growth rates, da/dN, for the shielding corrected data are plotted as a function of ΔK_{eff} after allowing for the effect of both crack bridging and closure (see text). Error bars on the small crack data represent the range of ΔK over the increment of measured crack growth.

4. PROGRAM ORGANIZATION AND PERSONNEL

The work described in this report was performed in the Department of Materials Science and Mineral Engineering, University of California at Berkeley, under the supervision of Dr. R. O. Ritchie, Professor of Materials Science, and Dr. A. W. Thompson, and aided by graduate student research assistants working for their M.S. degrees.

    i)   Professor R. O. Ritchie, Principal Investigator
             Department of Materials Science and Mineral Engineering

    ii)   Dr. A. W. Thompson
             Department of Materials Science and Mineral Engineering

    iii) Josh P. Campbell, Graduate Student Research Assistant
             Department of Materials Science and Mineral Engineering

    iv) Jamie J. Kruzic, Graduate Student Research Assistant
             Department of Materials Science and Mineral Engineering

    v)   Aindrea L. McKelvey, Graduate Student Research Assistant
             Department of Materials Science and Mineral Engineering

5. PUBLICATIONS

5.1 Refereed Journals

1. J. P. Campbell, J. J. Kruzic, S. Lillibridge, K. T. Venkateswara Rao, and R. O. Ritchie, "On the Growth of Small Fatigue Cracks in γ-Based Titanium Aluminides," *Scripta Materialia*, accepted for publication and in press, 1997.

2. J. P. Campbell, K. T. Venkateswara Rao, and R. O. Ritchie, "On the Role of Microstructure in Fatigue-Crack Growth of γ-Based Titanium Aluminides," *Materials Science and Engineering A,* accepted for publication and in press, 1997.

3. A. L. McKelvey, K. T. Venkateswara Rao, and R. O. Ritchie, "On the Anomalous Temperature Dependence of Fatigue-Crack Growth in γ-Based Titanium Aluminides," *Scripta Materialia*, submitted May 1997.

5.2 Refereed Conference Proceedings

4. R. O. Ritchie and K. T. Venkateswara Rao, "Cyclic Fatigue-Crack Growth in Toughened Ceramics and Intermetallics at Ambient to Elevated Temperatures," in *ECF-11 - Mechanisms and Mechanics of Damage and Failure,* Proceedings of the Eleventh European Conference on Fracture, J. Petit, ed., EMAS, Warley, U.K., vol. 1, 1996, pp. 53-69.

5.3 Theses

5. A. L. McKelvey, "High Temperature Fracture and Fatigue Crack Growth of a γ-Based Titanium Aluminide," M.S. Thesis, University of California, Berkeley, December 1996.

6. J. P. Campbell, "Room Temperature Fatigue-Crack Growth and Fracture Behavior in γ-Based TiAl Intermetallics," M.S. Thesis, University of California, Berkeley, December 1996.